Available online at www.sciencedirect.com
ScienceDirect
Journal of Magnetism and Magnetic Materials 307 (2006) 1–31
Journal of magnetism and magnetic materials
www.elsevier.com/locate/jmmm

Topical review

Advances in nanomagnetism via X-ray techniques

G. Srajer[a,*], L.H. Lewis[b], S.D. Bader[c], A.J. Epstein[d], C.S. Fadley[e,f], E.E. Fullerton[g], A. Hoffmann[c], J.B. Kortright[f], Kannan M. Krishnan[h], S.A. Majetich[i], T.S. Rahman[j], C.A. Ross[k], M.B. Salamon[l], I.K. Schuller[m], T.C. Schulthess[n], J.Z. Sun[o]

[a]*Advanced Photon Source, Argonne National Laboratory, Argonne, IL 60439, USA*
[b]*Center for Functional Nanomaterials, Brookhaven National Laboratory, Upton, NY 11973-5000, USA*
[c]*Materials Science Division, Argonne National Laboratory, Argonne, IL 60439, USA*
[d]*Department of Physics and Department of Chemistry, Ohio State University, Columbus, OH 43210, USA*
[e]*Department of Physics, University of California Davis, Davis, CA 95616, USA*
[f]*Materials Sciences Division, Lawrence Berkeley National Laboratory, Berkeley, CA 94720, USA*
[g]*San Jose Research Center, Hitachi Global Storage Technologies, San Jose, CA 95120, USA*
[h]*Department of Materials Science, University of Washington, Seattle, WA 98195, USA*
[i]*Physics Department, Carnegie Mellon University, Pittsburgh, PA 15213, USA*
[j]*Department of Physics, Carwell Hall, Kansas State University, Manhattan, KS 66506, USA*
[k]*Department of Materials Science and Engineering, Massachusetts Institute of Technology, Cambridge, MA 02139, USA*
[l]*Department of Physics, University of Illinois at Urbana-Champaign, 1110 W. Green Street, Urbana, IL 61801, USA*
[m]*Physics Department-0319, University of California—San Diego, La Jolla, CA 92093, USA*
[n]*Center for Nanophase Materials Sciences, Oak Ridge National Laboratory, P. O. Box 2008, Oak Ridge, TN 37830-6164, USA*
[o]*IBM Research, 1101 Kitchawan Rd., Rt. 134, Yorktown Heights, NY 10598, USA*

Received 5 April 2006; received in revised form 15 June 2006
Available online 22 August 2006

Abstract

This report examines the current status and the future directions of the field of nanomagnetism and assesses the ability of hard X-ray synchrotron facilities to provide new capabilities for making advances in this field. The report first identifies major research challenges that lie ahead in three broadly defined subfields of nanomagnetism: confined systems, clusters and complex oxides. It then examines the relevant experimental capabilities that are currently available at hard X-ray synchrotron light sources, using the Advanced Photon Source (APS) at Argonne as an example. Finally, recommendations are made for future development in X-ray facilities that will enhance the study of nanomagnetism, including new experimental directions, modifications that would enable in situ sample preparation, and measurements at high magnetic fields and/or low temperatures. In particular, in situ sample preparation is of high priority in many experiments, especially those in the area of surface magnetism.

Keywords: Magnetism; Nanomagnetism; Nanomagnetism and X-rays; Confined magnetism; Cluster magnetism; Phase-separated magnetic systems

1. Introduction

The present paper is a distillation of a workshop, entitled "Nanomagnetism Using X-ray Techniques" that was held in Fontana, Wisconsin, August 29-September 1, 2004, that was held as part of a strategic planning exercise sponsored by the Advanced Photon Source (APS) of the Argonne National Laboratory. The APS is a third-generation hard X-ray synchrotron source that serves as a major national user facility and is supported by the US Department of Energy. The purpose of the workshop was two-fold: first, to survey topics of current interest in nanomagnetism and identify emerging major themes. Second, to evaluate the role that X-ray techniques could play in addressing the fundamental research issues that lie ahead. Enhancing present X-ray capabilities and/or evolving new techniques to meet future challenges will assist both the synchrotron

*Corresponding author.
E-mail address: srajerg@aps.anl.gov (G. Srajer).

0304-8853/$ - see front matter © 2006 Published by Elsevier B.V.
doi:10.1016/j.jmmm.2006.06.033

X-ray science community in general and the APS in particular in planning for new instrumentation and resource priorities. The workshop was organized along three broad thematic areas in nanomaterials realm: confined magnetism, cluster magnetism, and complex oxide/phase-separated magnetic systems. We here first present an overview of grand challenges in nanomagnetics and then summarize the key basic and applied aspects of new nanostructured magnetic materials. The role that synchrotron X-ray techniques play in addressing the grand challenges follows. Finally, the paper ends with recommendations for future directions.

Nanomagnetism describes the science and technology underlying the magnetic behavior of nanostructured (1–100 nm) systems. It focuses on the magnetic behavior of individual building blocks of nanostructured systems as well as on combinations of individual building blocks that display collective magnetic phenomena. A fundamental understanding of nanomagnetism can be exploited to yield integrated systems with complex structures and architectures that possess new functionalities. Nanomagnetism provides new paradigms for condensed matter science. For example, there are differences in the temperature stability of a ferromagnetic state, spin polarization effects that can induce magnetic moments on nearby "non-magnetic" atoms, spin effects on quantum mechanical tunneling probabilities, the possibility of directing the movement of nanomagnets within individual living cells, the potential to detect pathogens through a combination of biological molecular recognition and magnetoresistive sensing using nanomagnetic thin films. Fundamental scientific questions common to the potential technological applications envisioned are concerned with the origin of magnetic couplings, spin transport across interfaces, spin-lattice interactions in complex materials and the magnetic domain configuration and dynamics arising from contact between different kind of magnets, for example antiferromagnets and ferromagnets.

2. Grand challenges in nanomagnetism

The grand challenges in nanomagnetism can be expressed in a number of ways depending on the audience [1]. At the most basic level the challenge is to create, explore and understand new materials that exhibit unexpected collective behavior, also known as emergent behavior. The creation of emergent matter energizes the synthesis community, and high-quality synthesis of new materials is critical to the future of all of condensed matter and materials physics. Nanoscience offers exciting new routes to create advanced materials and hierarchically assemble systems in a non-Edisonian manner. Utilizing the three basic tools of nanoscience—geometric confinement, physical proximity and self-organization—one can create materials by design. Confinement creates new properties from known materials via manipulation of dimensionality. Proximity effects allow multi-component composites to behave as new materials that embrace properties that are often mutually exclusive and thus not found in single-component systems. Self-organization utilizes rules of Nature to segregate and/or assemble systems on ultra-small length scales that transcend the limits of present-day lithographic definition. Self-assembly shows promise of becoming a powerful approach to miniaturize structures in an affordable manner with very high uniformity. A challenge is to utilize self-organization, as is accomplished in biological systems, to create not just component materials, but fully functional, integrated systems. One can imagine pulling an entire computer processor out of a test tube in the future. Achieving such goals certainly encompasses non-equilibrium synthetic routes, and the creation of multifunctional materials. Competing interactions and the preponderance of low-lying energetic states and quantum fluctuations help create the complexity that gives rise to unanticipated phenomena in magnetic nanosystems. We note that, during the exploration of magnetic surfaces, interfaces and multilayers undertaken a few decades ago, the discoveries of spin-valve read heads or magnetic random access memory was completely unanticipated. This realization underscores the fact that fundamental studies involving the creation of emergent matter is an important stimulant of advanced technologies.

The second grand challenge in nanomagnetism, beyond the creation of emergent matter, is the exploration of its magnetic properties. This task requires all levels of characterization tools. Essential in this is the utilization of the advanced user facilities that are available to the research community. This underscores an important synergy between materials creation and exploration that requires national investments both in synthesis and in major user facilities. Additionally, understanding emergent behavior requires the talents of the theory community and the utilization of high-performance computing to simulate complex behavior. This challenge has many facets. It includes: (i) defining the rules that govern self-organization; (ii) understanding spin dynamics and equilibrium states at the spatial and temporal limits of interest; (iii) understanding spin transport phenomena, spin-torque effects, spin accumulation, spin diffusion, etc.; and (iv) relating such effects to the detailed structure of the material. This challenge also involves understanding how to create entangled spin systems, and how to control the process as well as read the states. A longer-term aspect of the challenge is to foster communication of information via spin currents and excitations without the flow of charge. This would be a novel approach to complement existing electronic circuitry that depends on charge flow.

Why create, explore and understand nanomagnetic emergent matter? An important reason is that the more detailed understanding which is the goal of basic science will enable the community to address the strategic needs of our society at large. It is vital to stimulate the economy and create new jobs by ushering in new technologies and innovations. New diagnostic tools and treatments for diseases will preserve health and wellbeing, as well as

heal the ill and help the impaired. New sensors will help ensure homeland security, and advanced materials and approaches will provide for national defense needs. It is important to create materials and harness phenomena that will advance transportation requirements, and it is imperative to take leadership in meeting national goals of energy independence. Additionally, all of these initiatives must be advanced in a manner that is respectful of the environment. These are goals for the nanomagnetism community, for the nanoscience and nanotechnology communities, and for the larger materials research communities. The nanomagnetism community is in a particularly advantageous position to rise to these challenges because of the enormous potential derived from recent breakthroughs. Although magnetism is one of the oldest sciences known, it is a driving force in the new scientific era of nanotechnology. This statement is highlighted quite succinctly by examining the evolution of the giant magnetoresistance (GMR) effect, which made the transition from a laboratory curiosity to a technology driver within the short span of about ten years. From GMR, a host of new phenomena, materials, and potential technologies are blossoming. An overview of exciting aspects of magnetism research can be found in the collection of review articles entitled, Magnetism Beyond 2000 [2].

3. Magnetism in confined geometries

Magnetism in confined geometries is an active and vital area of research that will surely produce much new science and many applications in the next twenty years. In general, it is understood that systems with confined (or finite) geometries are those with dimensions on the order of the domain wall width, or of the mean free path of conduction electrons, i.e., nanometers. Confined systems that exhibit novel properties often consist of dissimilar materials that include at least one magnetic component (ferromagnetic, antiferromagnetic, etc.). Geometries of interest at the nanoscale include thin film heterostructures, superlattices, and nanostructured, nanopatterned or granular thin films. A topical review of the fabrication and properties of ordered magnetic nanostructures was presented by Martin et al. [3]. Arrays of nanoparticles and nanorods are discussed in Section 4. Although the future is difficult to predict, based on past experience, the area of confined magnetism is anticipated to produce breakthroughs in information storage, sensing and other spintronic applications.

The main areas of interest in the study of confined magnetism include: (i) confinement and quantization by the finite size, and (ii) the proximity effect due to the leakage of the electronic wavefunction and attendant magnetization outside of the physical bounds of the nanostructure. Since magnetism depends on a variety of length scales, quantitative structural characterizations must be made at a similar variety of scales. Relevant length scales and characterization tools are shown in Fig. 1 [4]. Examples of confinement-induced effects include vortex-state formation in magnetic nanodots, and modifications of the magnetic structure by surface defects. Proximity effect examples include coupling phenomena in Fe–Cr multilayers, induced magnetism in heterostructures built from nominally non-magnetic constituents, training effects in exchange-biased systems, and changes in the interfacial magnetization. To study such phenomena from both applied and basic science perspectives one needs access to probes that enable the:

- Mapping of the magnetization at nanometer length scales and sub-nanosecond time scales;
- Study of buried layers and interfaces;
- Element-sensitive structural, chemical and magnetic characterizations;
- Pump–probe experiments carried out under photonic, electronic and magnetic stimuli;
- Monitoring and control of collective excitations such as phonons, magnons, polarons and excitons.

Ideally the above studies would have the potential to be conducted under specialized environments, including ultra-high and ultra-low temperature, high pressure, and especially in variable magnetic fields up to 20 T. Furthermore, it is necessary to apply theoretical and numerical predictions of novel physics and effects of unusual geometries that extend beyond existing understanding. In particular, theoretical understanding of the interaction of X-rays with magnetic structures, especially in the presence of surfaces and interfaces and in conjunction with proximity configurations, is needed.

It should be stressed that the field of nanomagnetism is now beyond proof of concept. The time is thus ripe for applying sophisticated techniques to the solution of real physics-materials science problems that transcend simplifying assumptions. This requirement implies the ability to conduct detailed, quantitative studies that are correlated with materials growth processes and other physical property measurements. Selected examples will be used to highlight some of the scientific and technological issues that need to be explored in the area of magnetism in confined structures.

3.1. Lateral spin structures and transport

Understanding the transport of spins across interfaces in ferromagnetic (F) and non-ferromagnetic metallic (N) heterostructures is a fundamental challenge in the emerging field of spintronics [5,6]. The goal of spintronics, or magnetic electronics, is to explicitly utilize the spin of the electron instead of, or in addition to, the charge of the electron to communicate information. Spin-transport across interfaces gives rise to both the well-known GMR effect in F/N/F trilayers and F/N multilayers [7–9], and the recently discovered spin-transfer torque effects [10] in nanoscale F/N/F trilayers. To date most work has focused on vertical, or stacked, heterostructures; however, it is also promising to explore lateral, or patterned, heterostructures

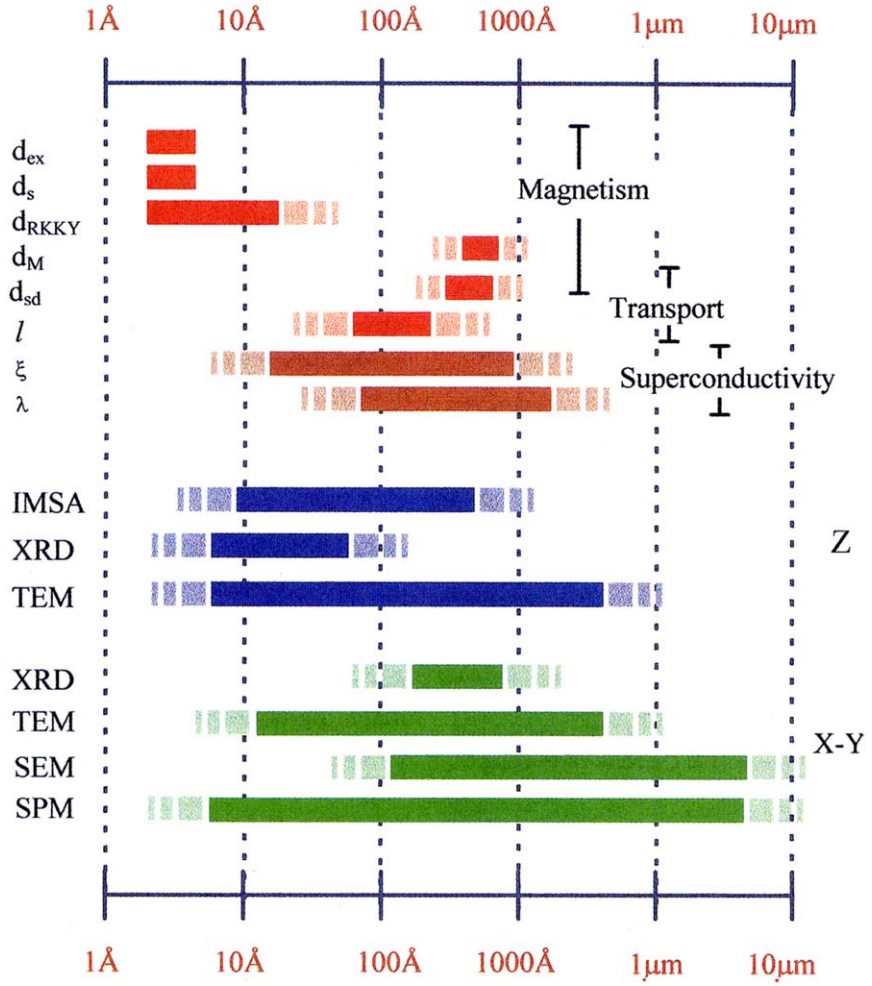

Fig. 1. Important length scales in magnetism and superconductivity and relevant characterization tools. The density of vertical lines indicates the reliability and range of applicability of the tool at a particular length scale. Taken from Ref. [4].

since they offer additional degrees of freedom to tailor desired properties. Additionally, future spintronic applications will require integration of a large number of devices where lateral spin-transport and spin-interconnection would be essential in order to achieve miniaturization, speed and cost-effectiveness. Furthermore, a planar two-dimensional (2D) geometry (see Fig. 2) has additional advantages [11–13] including flexibility in tailoring the magnetic properties of the ferromagnetic components through their shape anisotropy. More importantly, if the spin-polarization in the nominally non-magnetic component of the system may be imaged directly, i.e., via circular magnetic dichroism (see Section 6), then a real-space image of the spin-diffusion profile could be obtained [14]. This information may then be used to directly investigate spin-diffusion after spin-injection, and spin-imbalance as might occur from spin-Hall effects [15].

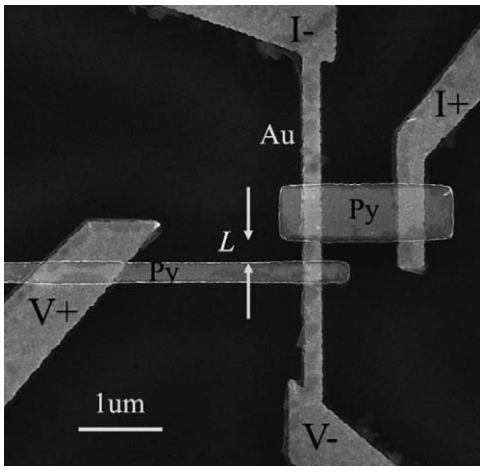

Fig. 2. Scanning electron microscopy of a permalloy/Au/permalloy lateral spin valve from Ref. [13].

3.2. Nanorings and nanopillars

Isolated confined structures, such as nanorings and nanopillars, provide the necessary architecture for exploring new phenomena, such as spin-transfer torque effects, as well as new technological applications, such as magnetic random access memories (MRAM). For such exploration to continue unabated, new physics needs to be realized in novel materials and structures made by new fabrication methods, and verified by advanced characterization tools.

A variety of small magnetic structures, including squares, rectangles, circular discs and rings have recently been studied [16–25]. Such structures can form a vortex state, in which the magnetic flux curls to form an internally confined state. However, there is a singularity at the center of the vortex where the magnetization points out of the plane. In the vortex state of a circular disc, the magnetic moments along circles of decreasing radii must rotate ever more sharply. The singularity at the center destabilizes the vortex state of the smallest circular discs that instead form into single-domain states.

The fundamental obstacles of vortex singularities in circular discs are removed in magnetic nanorings. Not only can a true vortex closure state be realized in this geometry, but magnetic nanorings have other unique attributes. A magnetic nanoring can acquire two distinct vortex states of opposite chirality, with magnetization circulating either clockwise or counterclockwise, in addition to bi-domain and other states containing domain walls. Each nanoring can therefore potentially store information as one or more magnetic bits. Magnetic rings have been created recently using electron-beam lithography [26–30]. The smallest rings reported are 90 nm in diameter and 30 nm in width [30]. The electron beam lithography technique is typically used to pattern relatively small areas, and the small number of rings in each array defies most magnetic characterizations except for the magneto-optic Kerr effect (MOKE) technique, resistance measurements, and in some cases, magnetic force microscopy. As an example, giant magnetoresistance measurements of Co/Cu/NiFe rings show that the soft NiFe layer reverses by a different mechanism in the multilayer compared to a single layer, due to magnetostatic interactions with the hard Co layer [31].

Recent synthesis methods create nanoring assemblages based on self-assembly, deposition, and ion beam etching without using electron-beam lithography [32]. A large number (10^9) of 100-nm nanoring magnets has been created over a macroscopic area (3 cm^2) with high areal density (45 rings/μm^2) while maintaining spatial and dimensional uniformity, as shown in Fig. 3. Because of the large number of near-uniform rings, the switching characteristics can be readily measured, by means of a vibrating sample magnetometer (VSM), and compared with micromagnetics simulations. Since the lateral dimensions of the nanorings are in the 100-nm range, traditional magnetic force microscopy (MFM), with a lateral resolution of 30–50 nm, is no longer adequate. Spin-sensitive microscopy is needed using X-ray photons or other means with a lateral resolution <3 nm.

Another example of a confined structure with novel magnetism is nanopillars. Current-induced magnetic reversal has been demonstrated in Co/Cu/Co multilayer spinvalve nanopillars [33] with particular relevance to MRAM devices. These pillars, synthesized by a novel fabrication process, possess lateral dimensions on the 100–200 nm scale. Depending on the applied field and its frequency, the current can cause in these pillars either

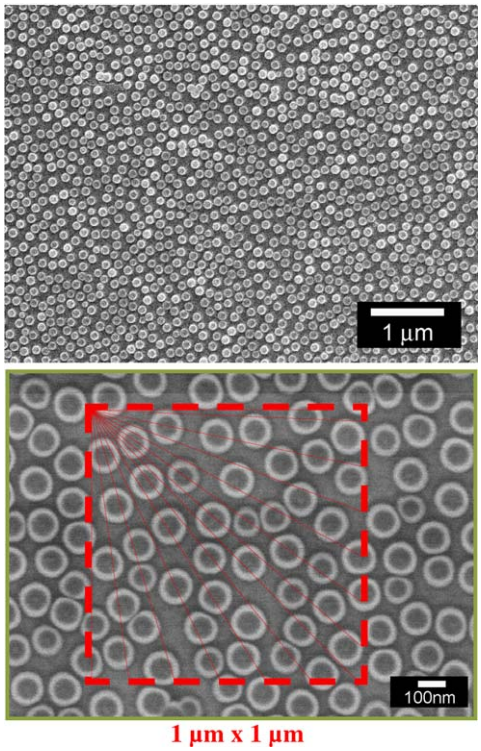

Fig. 3. SEM images of Co nanorings with an inner diameter of 100 nm (top) with a high areal density of 45 rings/mm^2 as shown in the lower figure. Based on Ref. [32].

magnetic reversal or precession, accompanied by the emission of microwaves at distinct frequencies [34,35]. Key to the full understanding of this effect is the determination of the dynamic behavior of the magnetization of the various layers in these structures on very short timescales and with high spatial resolution.

3.3. *Confined magnetic nanosystems for magnetic information applications*

Magnetic storage has played a key role in audio, video and computer development since its invention more than 100 years ago by Valdemar Poulsen [36]. In 1956 IBM built the first magnetic hard disk drive featuring a total storage capacity of 5 Mbytes at a recording density of 2 kbits/in^2. Since then the density of bits stored on a surface of a disk has increased by ~50 million fold to densities in 2005 of ~100 Gbits/in^2 and has been doubling every year over the past five years. At such densities, the bits must be positioned on the disk with nanometer resolution.

Presently, magnetic disk drives are based on longitudinal recording systems where the magnetization of the recorded bit lies in the plane of the disk. These systems contain a recording head composed of a separate read and write element, which flies in close proximity to a granular recording medium, as illustrated in Fig. 4. The recording media signal-to-noise (SNR) ratio needed for high-density recording is achieved by statistically averaging over a large number of weakly interacting magnetic grains per bit. The

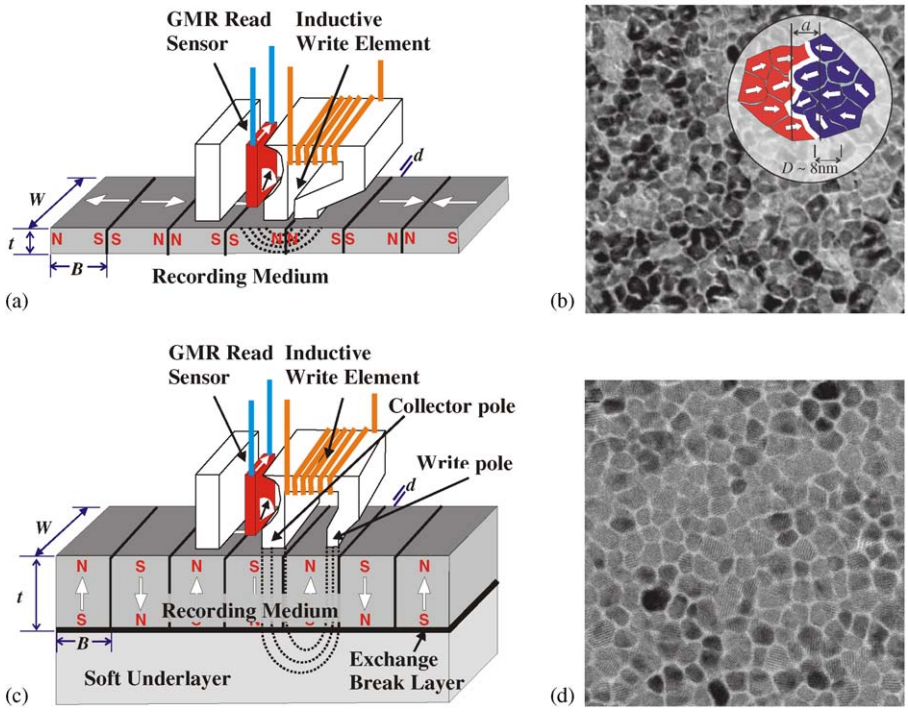

Fig. 4. (a) Schematic illustration of a longitudinal recording system with a read and write head flying above the recording medium. t is the medium thickness, W is the width of the recorded track, B is the bit size, and d the height the head flies above the medium. (b) Plan-view electron microscope image of a CoPtCrB magnetic alloy longitudinal recording layer. The amorphous grain boundaries are seen as white and the average grain size is 8.5 nm. Shown in the inset is a magnification of a transition region showing the interplay of the medium magnetic properties with the microstructure where D is the media grain size and the transition parameter a approximates the width of the magnetization reversal region. (c) Schematic illustration of a perpendicular recording system with a read and write head flying above the recording medium. The magnetization of the media is perpendicular to the films and a soft magnetic underlayer is below the medium to enhance the perpendicular write fields from the head. (d) Plan-view electron microscopy image of a perpendicular CoPtCr-oxide recording medium used to record data at 230 Gb/in^2 (see Ref. [43]). The average grain size is 6.3 nm with a coercive field of 6.4 kOe and a magnetic energy per grain of 75 k_BT.

granular microstructure limits the magnetic correlations to length scales comparable to the grain size and allows information to be written on a finer scale than possible in a homogeneous magnetic film. (Fig. 4b) This structure is currently achieved in CoCrPtB alloy thin films. When grown at elevated temperatures, these alloys phase segregate into high moment magnetic grains surrounded by non-magnetic boundary regions as shown in the TEM image in Fig. 4b.

The continued evolution of recording technologies towards higher areal densities is limited, in part, by enhanced thermal fluctuations that are manifest in the superparamagnetic effect [37,38]. Superparamagnetism describes the magnetic state of a system when ambient thermal energies (k_BT) become comparable to volume magnetic energies, resulting in a characteristic anhysteretic response for magnetic nanoparticles of sizes smaller than the typical domain size. This effect creates thermal instability in stored magnetic information and produces thermal fluctuations that add noise to sensors. Superparamagnetism is an issue that is well-understood yet still commands a high level of basic and applied research over 50 years after its initial introduction by Néel [37]. Continued growth of longitudinal storage densities has resulted from the development and characterization of magnetic heterostructures that help control magnetic interactions and correlations on the nanometer scale [39–42]. As storage densities continue to increase more dramatic changes in the media structure and system are required. The industry is now moving towards perpendicular magnetic recording shown schematically in Fig. 4c where the bits are stored perpendicular to the film surface. This allows for thicker and higher coercivity media which increase the energy stored in the grains. The materials of choice for perpendicular recording media of CoPtCr-transition metal oxide composite films for which the core of the magnetic grains consist of CoPt alloys and the oxide segregates to the grain boundary to isolate the grains (Fig. 4d) [43].

Beyond perpendicular recording, there are also new developments in thermally assisted recording, patterned media, and self organized magnetic nanoparticles. Determining the potential of these new structures (and the opportunities for magnetic X-ray studies) will occupy much research talent and require the capability in the future of characterizing magnetic materials at the nanometer spatial scale and sub-nanosecond temporal scale needed for future storage devices.

3.4. Patterned media from block co-polymers

The top-down synthesis strategy of lithography employing self-assembled block copolymers allows controlled fabrication of confined nanostructures with exceedingly regular features [44,45]. Such structures are of great interest for patterned media applications with high densities (e.g. periodicity <50 nm over large substrate areas). Diblock copolymers consist of polymer chains made from two chemically distinct, immiscible polymeric materials that are joined at one point. Self-assembly of these polymers allows formation of small-scale ordered patterns whose size and geometry depend on the molecular weights of the two types of polymer and their interaction [46–48]. Examples of block copolymer structures and associated magnetic data are shown in Fig. 5. Block copolymers have been employed as templates for the formation of magnetic nanoparticles by selective removal of one of the polymer types and use of the resulting template to pattern a magnetic film. The magnetic nanoparticle arrays made by this technique show strong effects of interparticle interactions as well as a magnetoresistance [49]. Structures such as aligned magnetic nanowires have also been made by electrodeposition into cylindrical channels in a block copolymer film [50]. Furthermore, the 2D arrangement of the structures on the surface can be controlled by shallow surface features, allowing long-range order to be imposed on the array [51]. This feature may enable the formation of practical data storage devices, such as patterned hard disks, a demonstration of which has already been presented [52].

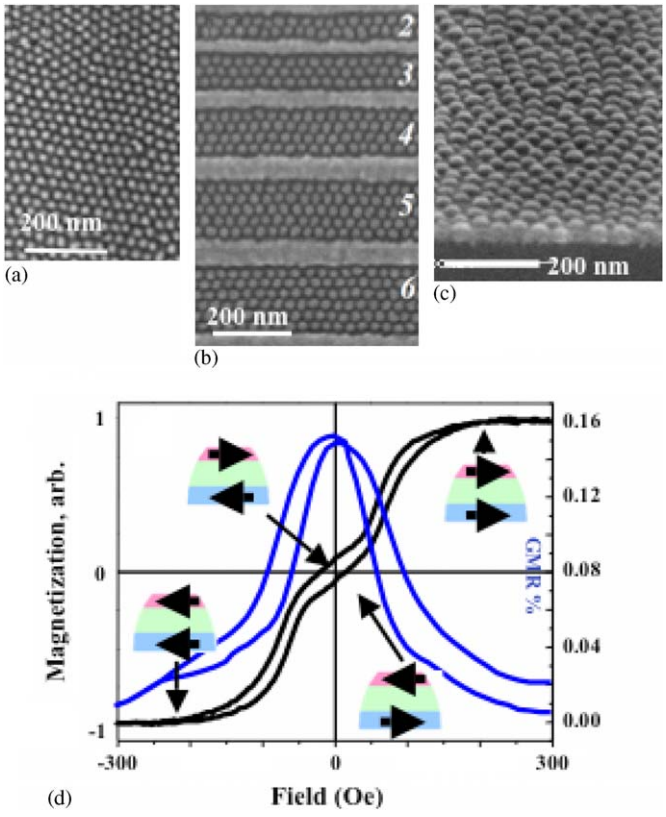

Fig. 5. (a) Self-assembled block copolymer on a smooth substrate, showing lack of long range order. (b) In shallow grooves, the polymer forms long range ordered structures. (c) Array of Co 'dots' made by block copolymer lithography. (d) Magnetization (black) and magnetoresistance (blue) of an array of 35-nm diameter dots made from a CoFe (3.3 nm)/Cu (6 nm)/NiFe (4.5 nm) multilayer. The multilayer structure is preserved during the fabrication process, and the data illustrate the separate switching of the NiFe and the CoFe layers. The insets show the magnetic state of the dots at each part of the hysteresis loop: the pink layer represents the CoFe and the blue the NiFe. Based on Ref. [49].

The challenges in this work include the understanding of: (i) the domain states of these small (<25-nm diameter) single or multilayer thin film elements; (ii) the reversal mechanisms and the dynamic behavior on sub-ns timescales; (iii) the interactions between particles and between layers in a multilayer particle; (iv) the origins of variability between nominally identical particles; and (v) how to relate these phenomena to the array geometry, the microstructure, the edge, interface and surface structure, the presence of surface oxides, and the shape and magneto-crystalline anisotropy.

3.5. Magnetic random access memories (MRAM)

MRAM is a new technology that employs a magnetoresistive device integrated with standard silicon-based microelectronics, resulting in a combination of speed, nonvolatility, and endurance not found in other memory technologies. The first generation of commercial MRAM went into production in 2006. Due to its unique combination of attributes, MRAM has the potential to be a universal memory that replaces several memory types. Since it is based on sub-micron magnetic devices, continued development of MRAM to smaller dimensions depends on advanced research in nanometer-scale magnetic structures.

Presently, materials research areas that are important to future generations of MRAM include: high-polarization materials, alternate tunnel-barrier dielectrics, and fundamental studies of specific electrode/dielectric combinations. Progress in these areas could enable higher performance MRAM at smaller dimensions by providing higher signal levels. For example, improved materials are needed to reduce variations in the tunnel barrier that in turn cause variations in the bit-to-bit resistance.

Writing data to MRAM cells involves switching the magnetic moment of the storage layer between two stable states. Fig. 6 shows a micromagnetic simulation of an MRAM bit switching [53]. Comparable experimental images on real MRAM bits would improve our fundamental understanding of magnetization reversal in these complex structures and help minimize the bit-to-bit switching variations observed in Mbit MRAM arrays. The development of methods for magnetic imaging, with nanometer-scale spatial resolution and sub-nanosecond time-resolved measurements, of magnetic switching would enable studies of switching dynamics in multilayer magnetic bits that cannot be accomplished by other methods.

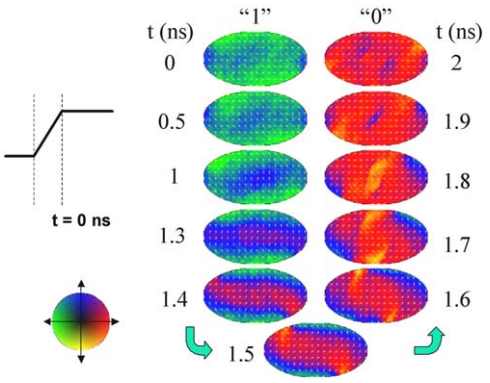

Fig. 6. Time-dependent micromagnetic simulation with random thermal fluctuations of a 4 nm NiFeCo MRAM bit patterned as a $0.6 \times 1.2\,\mu m^2$ ellipse. The current pulse was given a 2 ns rise time, and the element reversed within 2 ns. Based on Ref. [53].

A main challenge for MRAM to reach its full potential in the future is to continue to scale to smaller dimensions. Initially this will involve an evolutionary scaling of the present-day approach. As the leading edge of semiconductor lithography moves from 90 to 60 nm and then down to 35 nm, new architectures may play an important role. Possible candidates are bit-cells that exploit the recently discovered spin momentum transfer phenomenon that becomes most effective at dimensions <50 nm. While the switching of these structures has already been demonstrated, much work remains in materials research and fundamental understanding of nanomagnetics. Other new materials and magnetic device structures that enable switching at low currents with good data retention and higher read signals would have a large impact on the evolution of MRAM and its incorporation into the mainstream memory market.

3.6. *Interaction between spin-current and nanomagnets: spin-torque*

In a GMR or tunnel MR (TMR) device, spin-torque refers to the inverse action of a spin-polarized transport current on the nanomagnet traversed by such a current [54–58]. This interaction becomes important for devices <100 nm or so in size [59]. It manifests itself as a current-induced magnetic excitation and/or magnetic reversal of the nanomagnet. The interaction is important to understand, especially for applications, including memory technology, microwave generation, and recording head performance. For fundamental science, this is a new interaction between a spin current and a ferromagnet. It introduces a new mechanism for dynamic excitations [54,55,56,58,59,60–67] It also connects the magneto-transport problem to that of a magneto-dynamics problem [66–74], affecting our understanding of magnetic damping, spin-transport and spin-pumping in extended spin-circuits [66–79].

Fig. 7 shows an illustration of the spin angular momentum transfer process. When a charge current passes

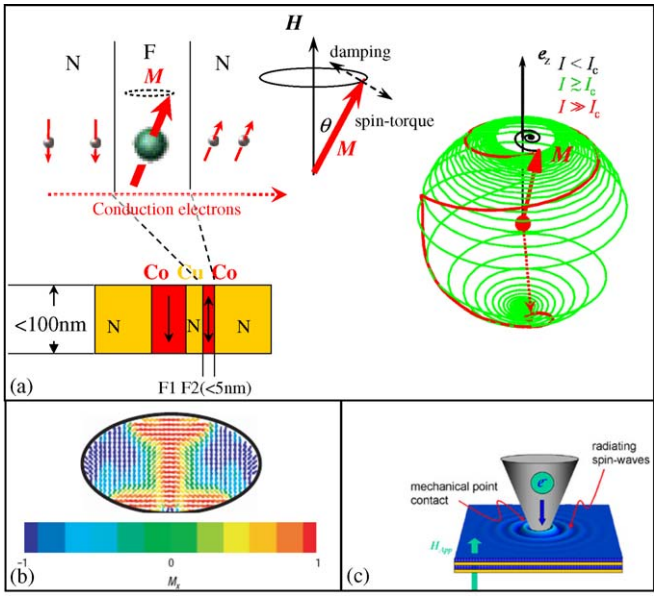

Fig. 7. (a) Illustration of the spin angular momentum transfer process, taken from Ref. [59]. (b) A nanostructured thin film pillar structure with a possible spatial distribution of the horizontal-direction magnetization at a time-sliced during reversal is shown using an extended Landau–Lifshitz–Gilbert equation-based finite element numerical simulation, taken from Ref. [75] (c) A concentrated charge current injection through a confined area can cause magnetic excitation and spin-wave emission, taken from Ref. [76].

through a spin-valve (or magnetic tunnel junction) stack as shown on the lower left of panel (a), the current becomes spin-polarized. The magnetic free layer (F2) will absorb some transverse spin angular momentum when repolarizing the spin-current, leading to an effective torque (spin-torque.) The direction of this torque can be parallel or antiparallel to the damping torque, depending on the sign of current and spin-polarization. When the direction of the spin-torque opposes the damping, a net increase in precession cone-angle may result if the amount of current supplied exceeds a certain threshold, leading to a precession state that can result in magnetic reversal as illustrated in the right side of panel (a) [59]. Fig. 7(b) shows a nanostructured thin film pillar structure, for which the magnetic state during spin-torque excitation and reversal can have a complex spatial distribution. One example of a possible spatial distribution of the horizontal-direction magnetization at a time-slice during reversal is shown. The result is obtained using an extended Landau–Lifshitz–Gilbert equation-based finite element numerical simulation [75]. Even for extended magnetic thin film multilayers, a concentrated charge current injection through a confined area (usually well below 100 nm in diameter) can cause magnetic excitation and spin-wave emission as shown in Fig. 7(c) [76].

For applications, a spin-torque introduces a unique handle on magnetic states, providing, for example, an efficient way of switching a nanomagnet's orientation via direct current injection. This approach is far superior to a

magnetic-field-write MRAM architecture in terms of low write-current and scalability to well below 45 nm nodes [57,59,60]. Spin-torque has also been demonstrated to generate microwave oscillations with narrow linewidths [63]. Such devices will have potential for communications and other applications that could benefit from a compact and tunable microwave source. The spin-torque interaction is also affecting the magnetic recording head's dynamic performance in a profound way [77]. Head devices, both spin-valves and tunnel junctions, will need to be optimized taking into account the effect of measurement current on the magnetodynamics and magnetic noise characteristics. Similarly, a spin-polarized current traversing a magnetic domain wall can also interact with it, causing domain wall motion, providing another interesting way of manipulating magnetic states of nanomagnetic structures [78–80].

Such magnetic states inducible by a spin-polarized current tend to have unique dynamics different from field-induced dynamics. High intensity, pulsed and tunable X-rays from modern (third generation) synchrotron sources do have the spatial and temporal resolution for the direct observation of these novel magnetic structures and for quantitative understanding of the element-specific magnetic dynamics.

3.7. Spin dynamics

A significant class of experiments utilizes optical pump–probe techniques to address spin dynamics in confined, interacting systems such as nanoparticle arrays. In these techniques, a sample is pumped by a pulse that generates an excitation. After a set period of time, a probe pulse characterizes the effects of the pump by means of transmission or reflection studies. In this manner spatial resolution of <300 nm can be achieved with ultraviolet light [81]. In cases where fast magnetic field pulses are generated with a strip-line, the practical time resolution is of order 50 ps [82]. This technique permits the study of magnetic excitations at long wavevectors ($q<2\times10^5\,\mathrm{cm}^{-1}$) and frequencies <10 GHz. Phenomena such as ultrafast switching [83,84], spin-wave localization [85,86], and vortex gyrotropic modes [87–89] in individual nanoparticles have been predicted and explored experimentally. Most of these systems are characterized by strong inhomogeneities in the internal magnetic field and/or in the magnetic microstructure. An example is shown [90] for a magnetic vortex in Fig. 8. This type of structure forms in cylindrical nanoparticles, in which the magnetization curls around the perimeter of the disk to minimize the magnetostatic energy, as mentioned in Section 3.2. A distinguishing feature of these structures is the existence of the vortex core in which the magnetization is forced to point out of the plane. Although this core cannot be resolved optically, it has a profound influence on the magnetization dynamics. As can be seen in Fig. 8, there is a node in the response at the center of the disk. Unfortunately, the spin dynamics in this core region cannot be readily explored using any existing experimental techniques. A similar technological limit has been encountered in recent experiments on ferromagnetic nanowires [91].

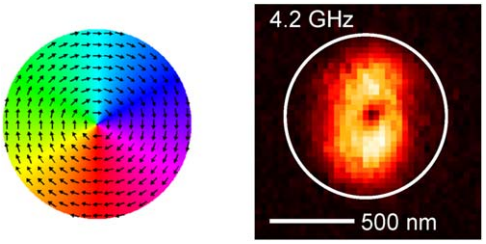

Fig. 8. A magnetic vortex schematic (left) and an experimental image based on the work by Park and Crowell in Ref. [90] of a spin-wave mode in a 1-μm diameter disk at 4.2 GHz. Note the dark spot (node) in the center of the experimental image. Accessing this region requires a probe with spatial resolution on the order of the exchange length (5 nm.).

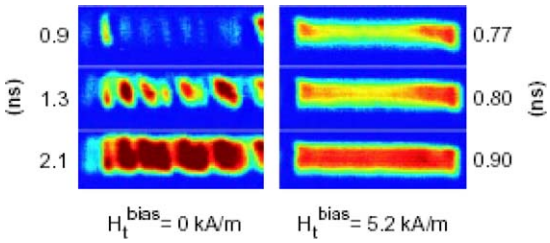

Fig. 9. Spatial profiles of the easy axis magnetization component measured at different time delays after a magnetic switching pulse was applied. The magnetization reversal mode is by incoherent rotation on the left, where the switching field is applied directly opposite to the initial direction of the magnetization. In the column on the right, the reversal is by quasi-coherent rotation, on account of the initial direction of the magnetization having been tipped away from the geometric and magnetocrystalline easy axis by a small transverse bias field. The field of view of each frame is 12×4 μm, and contains the entire 10×2 μm sample. The dynamic magnetic structure is full of details (spin waves, domain walls, vortex cores) on the nanometer scale and invisible to the magnetooptical probe used for this experiment. Taken from Ref. [92].

The type of excitation shown in Fig. 8 is predominantly magnetostatic in nature as the effects of exchange are relatively weak in this configuration. A second example with more complex dynamics is shown in Fig. 9 [92]. As the confining dimension decreases to the order of the exchange length ($\sim$ 5 nm), the fundamental character of the excitations should change. A time-resolved probe that enhances spatial resolution from the present level of $\sim$100 to <50 nm would improve our measurement capabilities, while a probe with 5-nm resolution would enable the exploration of fundamentally new physics. In order to fully exploit the advantages of improved spatial resolution, there should be an accompanying increase in the temporal bandwidth. If, for example, a measurement could be performed with 1 THz of bandwidth (i.e. 1 ps pulses) and 5-nm spatial resolution, then it would be possible to probe excitations that presently fall in the unexplored window of momentum space between time-resolved optical experiments and inelastic neutron scattering. This advance would permit time-resolved studies of quantum spin dynamics.

It should be stressed that these measurements rely on phase-coherent repetitive measurements. The data are obtained stroboscopically (utilizing ''boxcar'' averaging) and hence can only capture deterministic phenomena. This limitation means that currently laboratory experiments are not sensitive to many possible stochastic effects. Thus single-shot, time-dependent magnetic measurements, carried out at sub-nanosecond time scales and at nanometer length scales, would be important to characterize a greater variety of phenomena and should thus emerge as one of the important future nanomagnetism research directions. The ultimate goal for magnetic dynamics studies is to achieve 1 nm spatial resolution and <10 ps temporal resolution. Adoption of a sub-nanosecond ($\sim$100 ps) time resolution goal would be insufficient to probe precessional frequencies of 10's GHz, nor would it be able to track magnetization reversal by incoherent rotation which, at $\sim$1 km/s ($=1$ nm/ps), is not the fastest of magnetization reversal mechanisms [93]. Hence, there is a need for probes that can yield information about single-domain particles that ultimately cannot be described in the single-spin approximation [94]. This is the frontier at which the traditional Landau–Lifshitz–Gilbert model for dynamics becomes wholly inadequate, and at which the crossover to even smaller (cluster) magnetic systems naturally occurs. Synchrotron X-ray methods may hold special promise for such investigations because of their ability to yield element-specific information and because of the potential for combining high spatial and temporal resolution.

3.8. Theory and computation of confined magnetic systems

In the computational arena, magnetism and magnetic materials have been traditionally studied with phenomenological models. These models either work well or must be supplemented by new terms in the model to account for unexplained effects. While this empirical approach offers useful insight into the underlying science and provides benchmarks for the analysis of experimental data, it has its limitations. Chiefly the model may not be able to explain characteristics that depend on the details of the system at the nanoscale and may not have predictive capabilities.

Magnetic properties at interfaces and surfaces, which make up a large fraction of nanostructured and confined materials, are quite different from the bulk systems upon which many simple models are built. Model Hamiltonian approaches to magnetic nanostructures thus have limitations: either the Hamiltonian is too simple, based on bulk parameters that miss the essence of nanomagnetism, or the Hamiltonian is too complex and consists of many terms with unknown parameters that is unsolvable. It is fortunate that, the theory of magnetism and magnetic materials is already on a rather firm footing. Ab initio electronic structure methods are capable of predicting basic materials properties, such as the magnetization, magnetic anisotropy, the exchange energy, and the Curie or Néel temperatures. As computer performance increases and computational methods become more efficient, these first-principle methods can approach the point where substantial portions of nanostructures can be simulated without the need of fitting parameters (see also section 4.2.2. for more details). These methods will provide information beyond what is presently accessible experimentally on the following aspects: (1) atomic-scale magnetic structure in the interfacial and surface region of nanostructures; (2) nanomagnetism at short time and small length scales, and (3) understanding of the interaction of X-rays with magnetic nanostructures. It is important that theoretical calculations yield specific predictions that are experimentally accessible. Advanced models that are built on ab initio theory and experimental observation will lead to systematic advances in our understanding of nanomagnetism. The weaving together of theories that cover discrete spatial and temporal realms into a single hierarchical computational package remains a major challenge. The exploitation of quantum computation also appears on the horizon [95].

4. Cluster magnetism

Cluster magnetism describes magnetic phenomena found in nanoscale systems that are heterogeneous in all three spatial dimensions. The heterogeneity may have physical or chemical underpinnings and can exhibit a number of degrees of complexity. The specific topic of nanoscale thermodynamic heterogeneity that has recently been recognized to exist in a wide variety of complex oxides is covered in Section 5. The magnetic character of cluster systems depends on both the intrinsic properties of the individual clusters as well as on their interactions. These interactions determine the type of ordering within the system: the system heterogeneity may be regular, exhibiting either short- or long-range order, such as that found in self-assembled arrays of nanoparticles and molecules. Conversely, the system heterogeneity may be random, as that found in spin glasses, spin ice [96] and granular systems. An additional complexity is derived from the nature of the space between the clusters. The inter-cluster space may consist of organic polymer ligands, a matrix phase of insulating or conducting character, or vacuum. All of these factors ultimately determine the magnetic response and transport properties of the system.

The study and application of cluster magnetism is of great value from a number of perspectives. From a basic physics point of view, nanoparticle arrays and molecular magnets are test-beds for understanding the effects of nanostructuring, magnetic coupling, and of correlations from both static and dynamic perspectives. Superparamagnetism, discussed in Section 3.3, is an important phenomenon in nanoparticle arrays. As the scale of the system becomes smaller, superparamagnetism emerges at higher temperatures. This phenomenon has important ramifications for technological devices employing magnetic cluster systems, such as magnetic resonance imaging (MRI) contrast agents and recording media.

With rational synthesis it is possible to create uniform model nanoparticle systems that will foster understanding of emergent properties, especially in concert with theory and modeling. The science and practice of nanoparticle synthesis is steadily moving forward, to create a variety of shapes and geometries with unusual properties. While perhaps the best-known application is magnetic recording media, cluster magnetism may also expand the development of ultra-strong magnets for highly efficient motors, enable multifunctional sensors, and tailor superior soft magnets for electrical distribution. From a biological or biomedical point of view, magnetic clusters often cover the same size range as do biomolecules. This fortuitous coincidence cultivates interdisciplinary science between physics and biology as well as fosters new applications in pharmacology, medical treatment protocols and imaging.

Cluster magnetism review articles include the theory of fine magnetic particles [97], magnetic and transport properties of fine magnetic particles [98], and molecular magnets [99]. The objective of this section is to highlight forefront scientific issues regarding cluster magnetism and associated technological issues. In the following sections, recent advances are described in a select group of subtopics.

4.1. Molecular magnetism

Within the topic of cluster magnetism are organic-based or molecular nanomagnets, also referred to as single molecule magnets (SMM), which are a class of materials that exhibit a broad range of both conventional and new physical phenomena. SMM are distinct from inorganic-based nanoparticles by virtue of their constituent organic ligands that allow complete localization of the magnetic moments in the ferromagnetic atomic component. Molecular magnets contain a very large number (~Avogadro's) of magnetic molecules that are nominally identical, providing ideal laboratories for the study of nanoscale magnetic phenomena. Interest in these materials has grown dramatically in the last several years, owing to their possible use for high-density information storage, as well as the possibility that some members of this materials family could provide the qubits needed for quantum computation. An advantage of SMM over other potential quantum computer materials is that the nanoscale size of the individual molecules provides the ability to pack $\sim 10^{20}$ clusters into a cubic centimeter. Although there are no commercial devices based on organic-based magnets at present, it is anticipated that applications will be developed. For example, inexpensive, disposable, large-area MRAM made from self-assembled organic-based magnets and semiconductors could complement conventional inorganic-based electronic and magnetic materials.

SMM typically consist of monodispersed, nanoscale clusters of 2–15 magnetic core ions embedded in non-magnetic ligand groups. As one prototypical example, the full chemical formula for Mn_{12}-acetate is ($[Mn_{12}O_{12}(CH_3COO)_{16}(H_2O)_4]\cdot 2CH_3COOH\cdot 4H_2O$). These units are in turn packed into large single crystalline arrays. The magnetic core ions interact mainly through Heisenberg exchange interactions with intramolecular magnetic interaction strengths in the range 1–100 K, whereas the much weaker intermolecular magnetic interactions are ~10 mK in strength [100]. With molecular clusters of large total spin of 10 μ_B, Mn_{12} and similar molecular assemblages containing Fe_8 exhibit properties that straddle the border between classical and quantum magnetism. These clusters are magnetically bistable at low temperatures and exhibit macroscopic quantum tunneling between up- and down-spin orientations, as well as quantum interference between tunneling paths. Prototypical of the class [101], Mn_{12}-acetate contains magnetic clusters, shown in Fig. 10 that are composed of 12 Mn atoms coupled by super-exchange through oxygen bridges to provide a $S = 10$ spin magnetic moment that is stable at temperatures of the order of $\leqslant 10$ K.

The nominally identical, weakly interacting clusters are regularly arranged on a tetragonal crystal lattice. As illustrated by the double well potential of Fig. 11, strong uniaxial anisotropy yields doubly-degenerate ground states in zero field and creates a set of excited levels corresponding to different projections of the magnetization m_S, with $m_S = +10, +9 \ldots 0$, of the total spin along the easy c-axis of the crystal. Magnetic relaxation proceeds in these systems by spin reversal via thermal excitation over the anisotropy barrier and/or by quantum tunneling across the potential barrier. Below the blocking temperature $T_B \sim 3$ K,

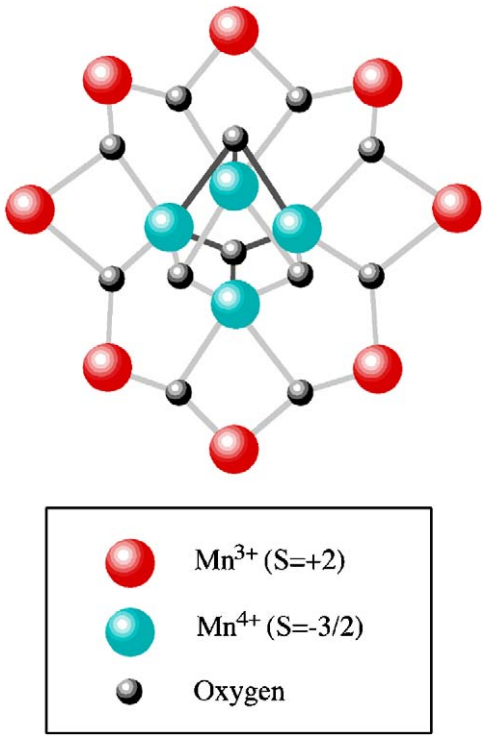

Fig. 10. Schematic depiction of the magnetic clusters in Mn12-acetate. Based on Ref. [101], courtesy of M. Sarachik.

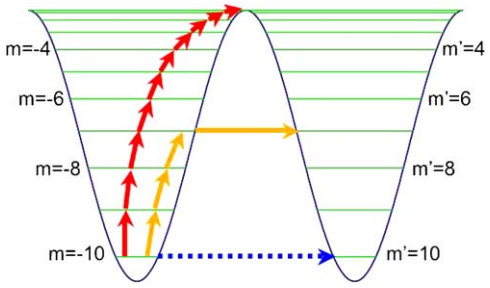

Fig. 11. Double well potential of Mn12-acetate weakly interacting clusters with doubly-degenerate ground states in zero field. Magnetic relaxation proceeds in these systems by spin reversal via thermal excitation over the anisotropy barrier and/or by quantum tunneling across the potential barrier. Based on Ref. [101], courtesy of M. Sarachik.

a series of steps appear in the magnetization M versus field H curves [102], indicating enhanced relaxation of the magnetization by tunneling whenever levels on opposite sides of the anisotropy barrier coincide in energy. Definitive confirmation of the quantum mechanical nature of the magnetic relaxation is provided by the demonstration in Fe_8 of quantum mechanical interference between different tunneling paths [103]. Because of their atomic level monodispersity, the energy levels of the quantum mechanical spin states are extremely well-defined, and Zeeman splittings in an external field have been accurately mapped. By choosing a field where two levels cross, it becomes possible to prepare a quantum mechanical superposition state, *i.e.*, an entangled state that is necessary for making qubits for a quantum computer. High spatial resolution polarized X-ray probes could be extremely useful for futures studies of such systems.

In another recent example, a number of SMM with magnetic cores consisting of just 2–4 magnetic ions have been prepared [104] and characterized. In these molecules, the transition-metal 3d-atoms (TM) link to each other via oxygen giving rise to a TM–O–TM super-exchange interaction with magnetic characteristics that depend on the TM–O–TM angle. The ligands also provide an opportunity for manipulating the nature and/or the strength of the exchange interaction. Results from ab initio electronic structure calculations [105] that identify the electronic configuration indicate that the density of the occupied and unoccupied electronic states are strikingly different. The electronic configuration governs exchange and super-exchange within the molecule. The calculations include anisotropy, which originates from the asymmetrical spatial location of the metal ions, and dipolar and exchange coupling between molecules in the crystal. Reversal of magnetization, which is sensitive to field magnitude, field scan rate, and temperature, is confirmed to occur via tunneling between energy levels that are aligned by an external field.

Organic-based or molecular nanomagnets are also important in the biological systems. For example, hemoglobin is an iron-containing respiratory pigment protein in blood that transmits oxygen from the lungs into tissues. This protein, which may be considered as a molecular nanomagnet, possesses a Fe–O bond length that is longer in the high-spin state than it is in the low-spin state. This feature means that the two spin states have different structures and therefore possess diverse chemical characteristics.

The benefit to society of successful development of organic molecular magnets is substantial. Implementation of new technologies will open up innovative means of addressing many needs including in electronics, energy consumption, health care delivery, and consumer packaging. Unlocking the potential of molecular magnets requires focused experimental and theoretical research. Topics for clarification include investigation of the existence of robust spin injectors, such as organic semiconductors and embedded inorganic magnetic nanoparticles, the possibility of magnetic organic, fully-spin-polarized semiconductors, and of photo-induced magnetism. For example, Figs. 12 and 13 [106] illustrate a spin-valve device in which the non-magnetic layer consists of an oriented carbon nanotube (CNT) array. These devices are intriguing, as many organic SMM arrays are transparent to

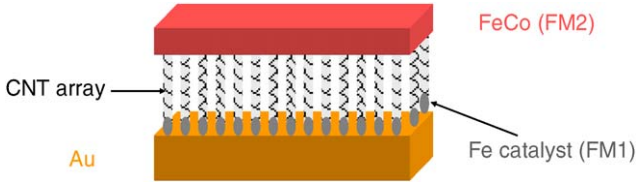

Fig. 12. Schematic illustration of a spin valve device employing carbon nanotubes. Courtesy of A. J. Epstein.

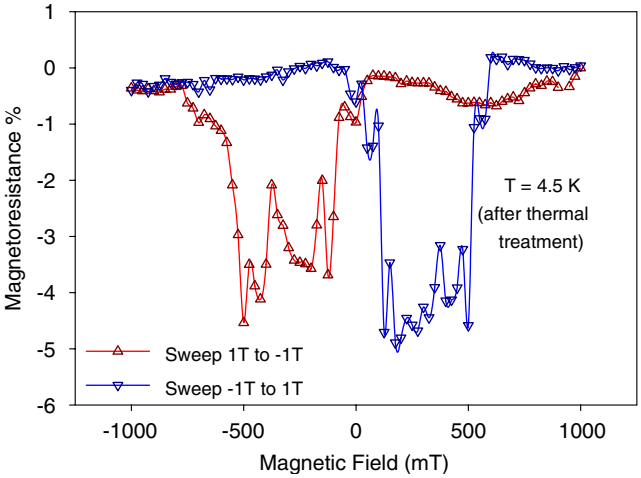

Fig. 13. Magnetoresistance—defined as $\partial R/R$ ($H = 1$ T) versus magnetic field for FeCo/Carbon Nanotube array/(Fe nanoparticle) spin valve device at 4.5 K. The negative magnetoresistance is obtained for a sample for which the FeCo layer was allowed to oxidize under ambient conditions for several weeks to form an oxide. The formation of an oxide at the interface between FeCo layer (as a result of aging and thermal treatment) and the CNTarray is the likely origin of the reversal of sign of the spin valve effect. Note the length of the CNTs between the Fe nanoparticle and the FeCo layer is ~7 μm. Taken from Ref. [106].

visible light, setting the stage for photo-induced magnetic phenomena. Open questions include the nature of the interfaces in SMM arrays, and clarification of the inter- and intra-cluster magnetic exchange coupling. Specifically, questions are centered on how electron spins in these systems traverse interfaces without losing their orientation.

4.2. Inorganic magnetic clusters

An area of great fundamental interest and critical technological need is the fabrication and magnetic property characterization of inorganic magnetic cluster arrays. Scientific challenges include understanding interactions and domain states of individual clusters and how these energies evolve when clusters are assembled into arrays. Additionally, the reversal mechanisms and the dynamic behavior of the array on sub-nanosecond timescales are of interest, as are the origins of the magnetic variability of nominally identical particles. It is necessary to relate these phenomena to the geometry microstructure and superstructure of the array, as well as to the shape and magnetocrystalline anisotropy, and to the presence of surfaces. Magnetic cluster arrays are of interest for a variety of applications, including exchange-spring permanent magnets, bio-detection devices, radiation sensors and patterned recording media.

4.2.1. Magnetic nanoparticle; synthesis and characterization

Self-assembly techniques involving solution chemistry comprise yet another method of inorganic nanoparticle and array synthesis [107]. Highly uniform, monodispersed, surfactant-coated nanoparticles form stable dispersions in alkanes or toluene. The consequences of this monodispersity is that the particles can then self-assemble into arrays [108] (see Fig. 14), just as atoms join to form close-packed fcc or hcp lattices when the solvent is evaporated, with slower growth processes leading to larger structural coherence lengths [109,110]. The size of the nanoparticles and the interparticle distance may be controlled via chemical variations. Superparamagnetic-to-ferromagnetic and insulator-to-metal phase transitions are expected as the interparticle distance is varied. Important issues related to self-assembly include understanding what kind of magnetically interesting structures can be formed, and what are the forces responsible. Interactions between particles, and between particles and a surface within a fluid, are understood on the micron scale but not on the nanoscale, where, for example, the notion of an electrostatic double layer surrounding a particle breaks down. There is a need for both experimental work and theoretical modeling in order to refine the understanding of these interactions. An important technological goal is the self-assembly of defect-free nanoparticle arrays over macroscopic length scales. Such arrays could be useful for data storage media, and can form more complex structures that might be useful in biomedical applications. The ability to study the dynamics of self-assembly will be critical to developing this understanding. Electrophoretic deposition of nanoparticles [111] will enable the nucleation, growth and melting of nanoparticle arrays to be driven using *ac*-electric fields. Small-angle X-ray scattering (SAXS) techniques can then assess the structural ordering length scale [112].

With standard surfactant coatings, the spacing between nanoparticles in self-assembled arrays is large enough that magnetostatic interactions dominate exchange. By changing the particle size and spacing, purely magnetostatic ferromagnetism has been observed in these structures [112]. The length scale of the structural ordering is also shown to be important; with a coherence length below ~300 nm, the nanoparticle assemblies show spin-glass-like behavior, while highly ordered structures act more like bulk ferromagnets [113]. An important research goal is to correlate the structural order and the nanoscale magnetization. SANS results show evidence of multiparticle magnetic correlations, but because large samples are needed, these experiments cannot be carried out on arrays with small numbers of layers. The unusual preference for arrays with an odd number of layers [114], as shown in Fig. 15, provide information about the layer-by-layer magnetization pattern. Early resonant soft X-ray scattering studies have

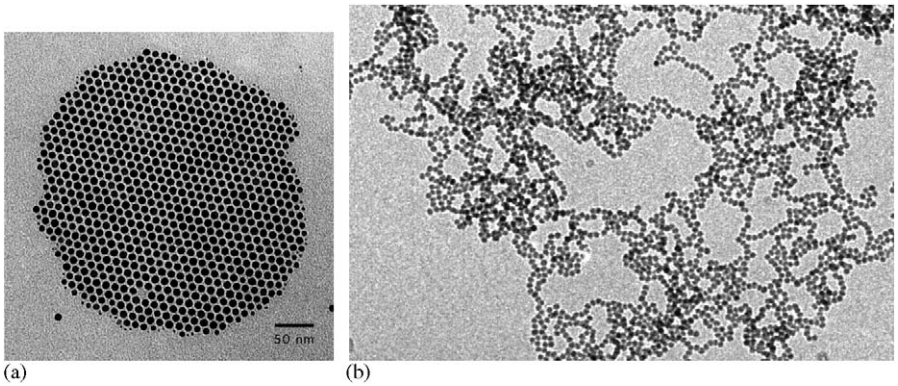

Fig. 14. (a) TEM image of 9 nm Co nanoparticles in an array self-assembled from a hexane dispersion. (b) TEM image of ~10-nm Fe_3O_4 nanoparticles in a magnetic gel self-assembled from an aqueous dispersion. The forces guiding self-assembly on this length scale are not yet sufficiently understood to make arrays of magnetic particles like (a) from aqueous dispersions, even though this could be useful for nanoscale bioassays, taken from Ref. [108].

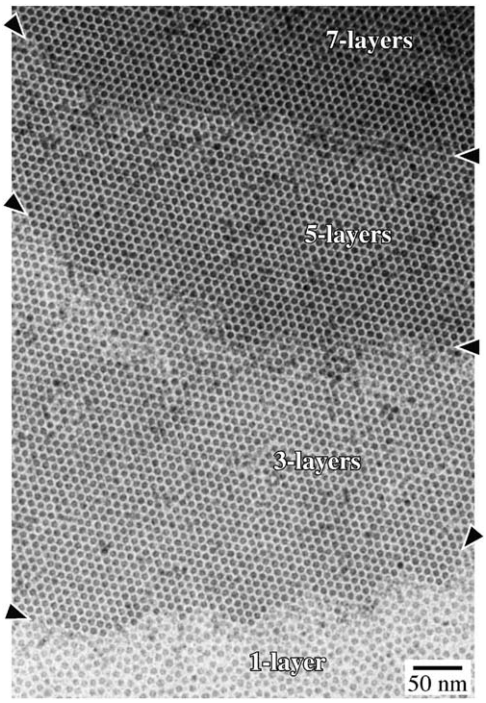

Fig. 15. Arrays of 6 nm Fe nanoparticles showing an hcp lattice and a preference for an odd number of layers. [114].

shown that it is possible to isolate pure magnetic scattering reflecting average interparticle moment orientations, and analyze these to understand the significance of dipolar interparticle interactions, even in superparamagnetic assemblies [115]. The large resonant cross-sections enable X-ray techniques to study assemblies as thin as one particle layer. These capabilities will be useful in evaluating the degree of exchange coupling of nanoparticles, either to each other or to other magnetic structures in nanoscale devices.

4.2.2. *Computational foundation of cluster magnetism*

Fundamental to understanding the magnetic behavior in clusters is the evolution of the magnetism as the structural scale descends from the bulk to the nanoscale. It is well established from decades of research that interface magnetism can be quite complex and different from bulk magnetism. Due to reduced symmetry, the magnetic anisotropy can be orders of magnitude larger than in the bulk. This result can lead to magnetic frustration and reorientation of the magnetization at the surface and interface. Furthermore, interfaces between dissimilar materials can change their individual properties. For example, when in contact with an antiferromagnet, the properties of a ferromagnet change dramatically; the coercive field is enhanced and, the magnetization curve can become asymmetric showing the exchange bias effect [116–118]. In nanoscale magnetic clusters, interface effects are expected to be even more significant as the interface region is a dominant part of the entire structure. For example, in an FePt nanoparticle of 6-nm diameter, ~40% of the atoms are located within one lattice constant of the surface. Indeed, surface segregation and surface magnetism are then expected to have a dominant effect on the magnetic state. Kodama et al. [119,120] found that the increase in coercive field of $FeNi_2O_4$ nanoparticles over that of the bulk is due to a spin-glass-like surface spin structure to which the ferrimagnetic core of the particle couples. Understanding the complex atomic spin structure of magnetic nanostructures is thus essential to the mastering of nanomagnetism itself.

Measuring the non-collinear magnetic state of a nanostructure is a difficult task since most experimental probes of magnetism average over length scales of $\geqslant 10$ nm. Information about the atomic-scale spin structure is usually inferred by comparison with model calculations. In many nanoscale systems, however, calculations cannot be based on bulk models, since parameters such as exchange and anisotropy constants, as well as the composition profile and atomic valence, are no longer similar to their bulk values. Model calculations, therefore, must be based on first-principles computational techniques that require input only of the atomic number, and are capable of predicting non-collinear magnetic states, atomic moments, dynamics and the response to external stimuli.

Methods to calculate the electronic structure [121] of magnetic nanosystems are mostly based on the local spin-density approximation [122] (LSDA) to density functional theory (DFT) [123]. These methods have proven to be reliable in predicting ground state properties, such as magnetic moments and anisotropies [124],as well as to calculate the temperature of magnetic phase transitions [125]. Extensions of the LSDA to study the dynamics [126] of non-collinear spin systems (in particular constrained LSDA) [127,128] are now available. Such efforts have been successfully applied to predict non-collinear spin structures of complex antiferromagnets such as FeMn [129,130] as well as the role of induced moments on high susceptibility elements such as Pt and Pd, or to calculate the effects of Ru on the magnetic exchange and anisotropy in FePt, CoPt, and FeRu [131,132], and reorientation transitions in thin films [133]. Furthermore, the application of orbital dependent functionals have matured to the point where it is now possible to reliably treat from first principles strongly correlated magnetic systems, such as manganites [134] and dilute magnetic semiconductors [135].

In recent years, the development of order-N electronic structure methods and their implementation on modern high performance computing hardware [136] have made possible simulations of non-collinear spin systems with thousands of atoms in the unit cell. With these capabilities, it is possible to show, for example [137], that the spin-structure of FeMn in a Co/FeMn thin film heterostructure reorients from the bulk 3Q structure into a quasi-1Q structure in the thin film with preferential moment directions perpendicular to the ferromagnetic Co moments (Fig. 16). Present-day calculations are already large enough

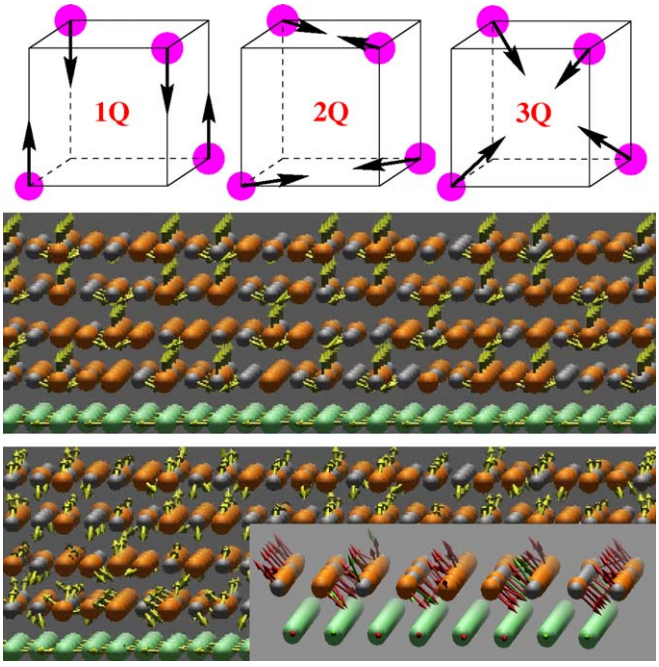

Fig. 16. *Upper panel*: three spin states consistent with neutron scattering measurements of δ-FeMn. Mössbauer spectroscopy indicates that the 1Q state is not present, while first principles calculations show that the 2Q and 3Q states are the only stable states. The latter is energetically the most favorable. *Middle panel*: starting spins configuration for a first principles calculation of a FeMn/Co multilayer. Co (green) is assumed to be in a ferromagnetic state while FeMn is initiated in a perfect 3Q state. *Lower panel*: final configuration after full relaxation of the magnetic state. Co atoms are still perfectly ferromagnetically ordered. The spin structure of FeMn has rearranged and resembles a 1Q state with Fe and Mn moments aligned perpendicular to the Co moments.

to allow prediction of magnetic ground state properties of nanostructures. It is expected that computer performance will increase by a factor of 100–1000 in the next five to ten years. With these advanced capabilities it will be possible to study finite temperature properties and dynamics of the magnetic state in nanostructures, for example nanoparticles of 5–10 nm diameter consisting of 5,000–20,000 atoms. On vector computers with $\sim 10^4$ fast vector processors, it will be possible to integrate the Landau Lifshitz equation [138] in which the effective fields and the magnetic moments are computed in first principles electronic structure calculations. On massively parallel computers with $>10^5$ super scalar processors, it will be possible to calculate temperature-dependent magnetic free energies of nanoparticles with ab initio Monte Carlo techniques. In these approaches, the energies of individual spin configurations are calculated with first principles electronic structure methods, and novel Monte Carlo techniques [139] are used to sample configuration space, thus enabling calculation of the entropic contribution to the free energy. Due to the dominance of magnetic fluctuations at the atomic scale, incorporating temperature and dynamics effects in predictions of magnetic properties is crucial for understanding nanostructures.

4.3. Magnetic clusters for biomedical applications

Magnetic nanomaterials provide opportunities for diagnostics and therapeutics for both in vivo and in vitro applications in biomedicine. The size scale of nanoparticles—similar to that of common biomolecules (< 50 nm)—makes them interesting for a wide range of biomedical applications [140] that includes intracellular tagging, contrast agents, antibody targeting and hyperthermia protocols [141]. For reference, size ranges of biological entities are given as follows: proteins (5–50 nm); genes (2 nm × 10–100 nm); viruses (20–450 nm) and cells (10–100 μm). The combination of biology and magnetism found in this arena is useful, because the biochemistry enables a selective binding of the nanoparticles, while the magnetism renders them easy to manipulate. Moreover, the absence of ferromagnetism in most biological systems allows the signal from magnetic nanoparticles to be readily detected with low noise. Directed drug delivery can be accomplished with magnetic nanoparticles: a drug is bound to a magnetic particle and either DC-magnetic fields are used to confine the drug in a specific location of the body, or ac-magnetic fields are used in order to trigger the release of the drugs. Key challenges for nanoparticles engineered for biological applications include the modification of nanoparticles for enhanced aqueous solubility, biocompatibility or bio-recognition, optimization of their magnetic properties including their relaxation dynamics over a broad range of frequencies and applied fields. For example, contrast in MRI is produced when magnetic nanoparticles modify the magnetic relaxation of the surrounding tissue. In addition to surface functionalization [142], nanoengineering of particle surfaces to optimize both their magnetic and optical response is important for diagnostic and therapeutic applications.

Hyperthermia involving the controlled heating of tissue employing magnetic nanoparticles to promote targeted cell destruction has the potential to be a powerful cancer treatment. Engineering superparamagnetic nanoparticles to yield the appropriate heat generation under AC magnetic field excitation is a complex process, highly dependent on particle size, crystallinity and shape. Investigation of magnetic heating parameters suitable for biological applications involves particle size and magnetic anisotropy optimization as well as studies of the complex magnetic susceptibility, heat capacity and power dissipation. Magnetic nanoparticles coated in a lipid bilayer, known as magnetoliposomes, can combine heat therapy with drug delivery to provide a synergistic treatment strategy. Magnetic particles can be injected into a patient and guided to a target site with an external magnetic field and/or specifically bind to target cells via recognition molecules coated onto the surface of the particles. Optimum performance requires control over the synthesis of the nanoparticles and their surface modification. While biomcompatible iron oxide nanoparticles are the materials of choice for these applications, specific applications call

for higher-moment cobalt nanoparticles. To this end, a synthesis route was recently developed involving the rapid decomposition of metallorganic precursors in a surfactant environment to prepare cobalt nanocrystals with tailored sizes (diameter ~5–25 nm) and controlled shapes, such as spheres or disks [143,144] as shown in Figs. 17 and 18. A surfactant coats the particles during synthesis and plays a key role in the nucleation and growth of the particles and their geometry. For example, disk-shaped nanoparticles are obtained by judicious choice of surfactants that adhere selectively to certain crystallographic planes promoting anisotropic particle shapes. While as-synthesized particles are initially hydrophobic, coating the particles with a second lipid layer (1,2-dipalmitoyl-sn-glycero-3-phosphocholine [DPPC]) is an effective route to make them hydrophilic and biocompatible [141].

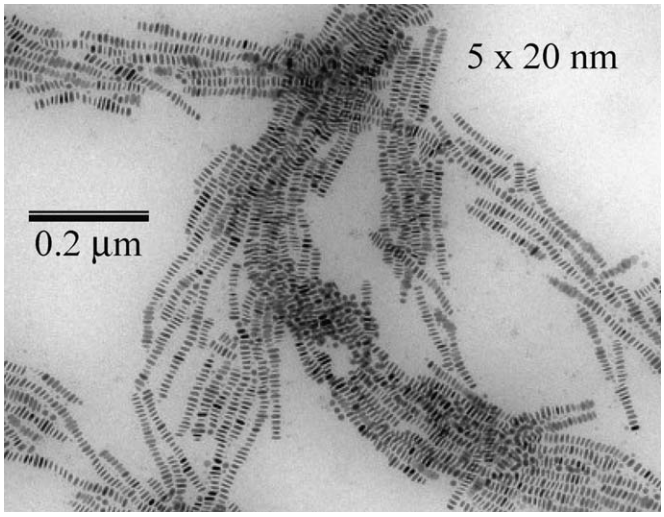

Fig. 17. TEM micrograph of self-assembled cobalt nanodisks: lyotropic liquid crystals. Based on Ref. [143].

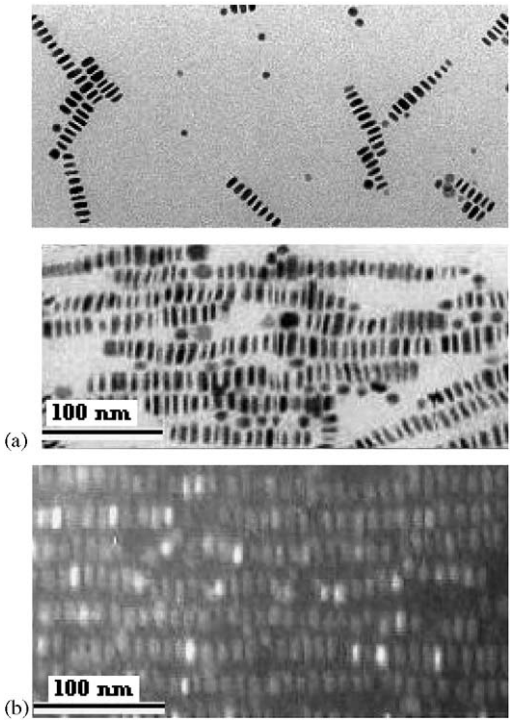

Fig. 18. Enlarged views of cobalt nanodisks. Based on Ref. [144].

The preparation of biologically functionalized magnetic nanoparticles can be quite challenging [145]. A novel approach to the creation of appropriately sized particles is to utilize viruses as inert molds for the nucleation and growth of magnetic nanoparticles [146,147]. A virus has a rigid container (the capsid), constructed from various proteins. This capsid contains the DNA that the virus injects into a living cell to replicate itself. For some of these viruses it is possible to remove the DNA, leaving behind an intact and inert capsid shell (ghost virus). The empty capsid can subsequently be used as a template for fabricating magnetic nanoparticles via precipitation from solution. This synthesis strategy has been demonstrated [148] for iron oxide and metallic cobalt nanoparticles using T7 bacteriophage, which produces nominally spherical particles of 40-nm diameter, Fig. 19 [149]. The magnetic nanoparticles fabricated by this procedure (“magnetic viruses”) have several key advantages to other magnetic nanoparticles fabricated using more traditional pathways. As all the viral particles are identical, they present a uniform template for the growth of the magnetic nanoparticles resulting in a very narrow size distribution. Furthermore, the size and shape of the particles can be varied by using different virus templates. Magnetic viruses can be engineered to express the desired biological functionality, since phage display libraries (collections of many different viruses with slightly different DNA) can be utilized to select viruses with the required affinity for the target of choice [150]. In addition, virus capsids are inherently biocompatible and thus ideally suited for in vivo applications.

The magnetism of small iron-based clusters may also lead to new diagnostic capabilities of neurodegenerative disorders, particularly Alzheimer’s disease (AD), Parkinson’s disease and Huntington’s disease.[151–153] It is known that patients with these diseases experience a disruption of normal iron metabolism, with total iron levels in diseased brains being significantly higher than in healthy ones. Cellular iron storage takes place in ferritins, a family of iron-storage proteins that sequester iron inside a protein coat as a hydrous ferric oxide–phosphate mineral similar in structure to the non-magnetic mineral ferrihydrite. A likely explanation of the elevated iron levels in affected brains is due to increased iron loading of the ferritin cores. In normal ferritin, a rigid protein shell surrounds an 8-nm-diameter cavity partially filled with ferrihydrite, with extra room in the cavity to accommodate additional iron. Recent findings [154,155] show that increased iron loading in brain tissue ferritin may lead to the formation of magnetite, a ferrimagnetic mineral that has Fe^{2+} ions, in contrast to the Fe^{3+} ion found in ferrihydrite. This biomineralization transformation

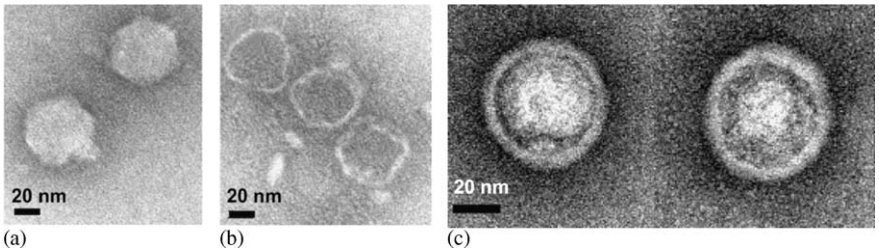

Fig. 19. TEM images of T7 bacteriophage. (a) normal viruses, (b) ghost virus particles after osmotic shock, and (c) "magnetic viruses" with iron oxide nanoparticles at their center; taken from Ref. [149].

involves the reduction of Fe^{3+} to Fe^{2+} and may be accompanied by toxicity and the production of free radicals associated with the presence of Fe^{2+} ions, believed to underlie oxidative stress and neuron damage. Studies of the ferritin-to-magnetite transformation using a series of AD and control tissue samples indicate a striking correlation between the amount of magnetite present and the progression of the disease.

5. Complex transition-metal magnetic systems

Despite a long history of research starting soon after WWII, there is a resurgence of interest in multi-element transition-metal magnetic compounds that exhibit electronic and magnetic phase transitions driven by a variety of parameters such as magnetic field, pressure and temperature. This is largely due to the discovery of the colossal magnetoresistance (CMR) effect [156,157]. CMR involves increased conduction electron mobility upon aligning the core spins in a magnetic field. The sensitivity of the magnetic transition to physical perturbations implies a strong coupling between charge, spin and lattice degrees of freedom, thus illustrating the sensitive nature of the *d*-shell electronic states to small changes in the atomic environment. Prototypical examples of these and related materials include the perovskite-structure manganites and cobaltites [158,159], as well as high-T_c cuprate [160–162] and ruthenate [163] superconductors. In his seminal book, Magnetism and the Chemical Bond [164] (1963) Goodenough quantified the connections between orbital occupancy and geometry and the resultant magnetic character in TM compounds, notably in TM oxides and chalcogenides. Since that time a profusion of important discoveries have been made concerning the rich variety of magnetic phenomena and transformations in this family of materials [165–167]. Recently, the ability to synthesize new, nanostructured complex materials and probe their electronic states and dynamic response has deepened our understanding as well as opened fresh questions. In particular, new discoveries concerning the interplay of closely spaced energies—thermal, magnetic, electrostatic—reveal unexpected ground states. In some cases electronic disproportionation takes place on the nanoscale, leading to a multiphase state that has only a very subtle chemical signature, if at all.

Complex TM magnetic systems raise a wealth of fundamental questions and possess undeveloped technological potential. Clarification of the thermodynamic underpinnings of the ground state of the material is key to understanding its behavior. Many complex, strongly correlated systems exhibit quantum phase transitions, i.e., they undergo a phase transition at zero temperature as some parameter is varied. This zero-Kelvin state [168], is found in systems that exhibit critical phenomena, including critical points and critical end points of various sorts, higher-order critical points, and entities coexisting in distinct phases. In such systems susceptibilities diverge despite the fact that only short-range correlations exist. Furthermore, the low-energy properties of the system are dominated by extremely rare configurations. Questions of theoretical interest include whether this phase separation constitutes a true thermodynamic state, and how the phase transition percolates throughout the system. Additionally, it is important to determine to what extent scaling works, and whether the phase separation has temporal characteristics of interest. In addition to quantum phase transitions, complex systems have recently been confirmed to exhibit subtle phase coexistence that is thought to underlie their phase and electronic transport properties [158,169–171]. Basic questions about these states persist, such as what is the size of the phase regions, and how does one control the size and morphology? The extent of local chemical variation remains unknown, as does the role of strain, disorder and lattice defects. It is of profound importance to identify structural precursors to phase separation in this family of materials.

Multiple degrees of freedom in complex systems can give rise to multiferroic phenomena, whereby a material may exhibit simultaneous ferromagnetism, ferroelectricity and ferroelasticity, subjected to specific crystal symmetry constraints [172]. The functionality of this class of materials extends beyond that of spintronics since they possess the potential of their parent form as well as crossover effects, permitting an additional degree of freedom—multifunctionality—in device design. Possible devices employing these novel materials include multiple-state magnetic elements, electric-field-controlled magnetic resonance devices, and transducers with magnetically modulated piezoelectricity. Furthermore, there is great technological interest in complex TM magnetic systems.

This is due to the collection of extraordinary functional phenomena that occur in the vicinity of the magnetostructural phase change, which are manifestations of the highly-correlated electron behavior. It may be that material inhomogeneity underlies these phenomena. In oxides, these phenomena include the CMR effect found in the hole-doped (La,Sr)-based manganites [173], of interest for magnetic sensors and the giant magnetocaloric effect (MCE) that is under development for CFC-free magnetic refrigeration [174,175].

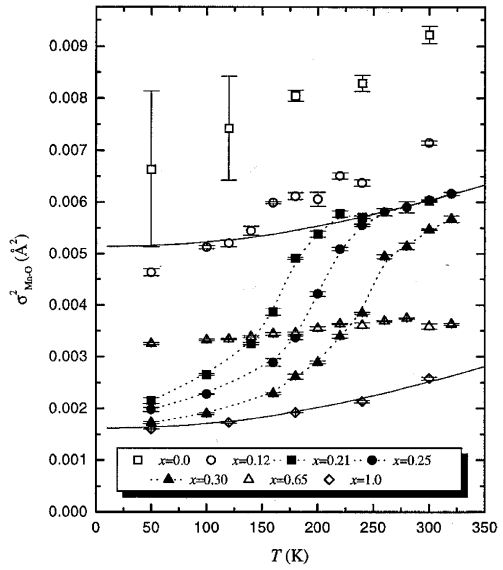

Fig. 20. Width of EXAFS peaks in $La_{1-x}Ca_xMnO_3$ for various concentrations x. The increase in width reflects the formation of polarons at high temperature. Dotted lines are guides to the eye. Relative errors are estimated to be smaller than the symbols, except for $LaMnO_3$. Taken from Ref. [178].

5.1. Fundamental properties: phase separation and griffiths phase in doped manganites

The CMR of the prototypical compound $La_{2/3}M_{1/3}MnO_3$ (where M is a divalent element, such as Sr, Ca or Pb) involves a percolation-like mixture of ferromagnetic/conducting and paramagnetic/resistive phase regions [176]. Evidence of this is provided in Fig. 20 depicting the local atomic environment as quantified by EXAFS (extended X-ray absorption fluorescence spectroscopy) [177,178]. The width of the EXAFS peaks, related to the distribution of Mn–O bonds in the $La_{2/3}M_{1/3}MnO_3$, decrease with increasing substitution level and show a distinct transition from shorter bonds to longer bonds with increasing temperature.

The evolution from a large bond length distribution, distorted by the Jahn–Teller interaction, to a smaller bond length distribution (undistorted) is obvious. From measurements of heat capacity and resistivity, it is possible to directly extract the proportions of conducting and insulating regions as functions of magnetic field and temperature as shown in Fig. 21 [179].

Unlike a conventional percolation picture, the metallic fraction in $La_{2/3}M_{1/3}MnO_3$ changes significantly with both temperature and field. A model that describes the approach to the phase transition with decreasing temperature was first presented by Griffiths [180], and leads to what is termed a Griffiths singularity. Within this context, at any temperature, pre-existing ordered regions are coalesced into clusters. As the temperature is lowered, the clusters

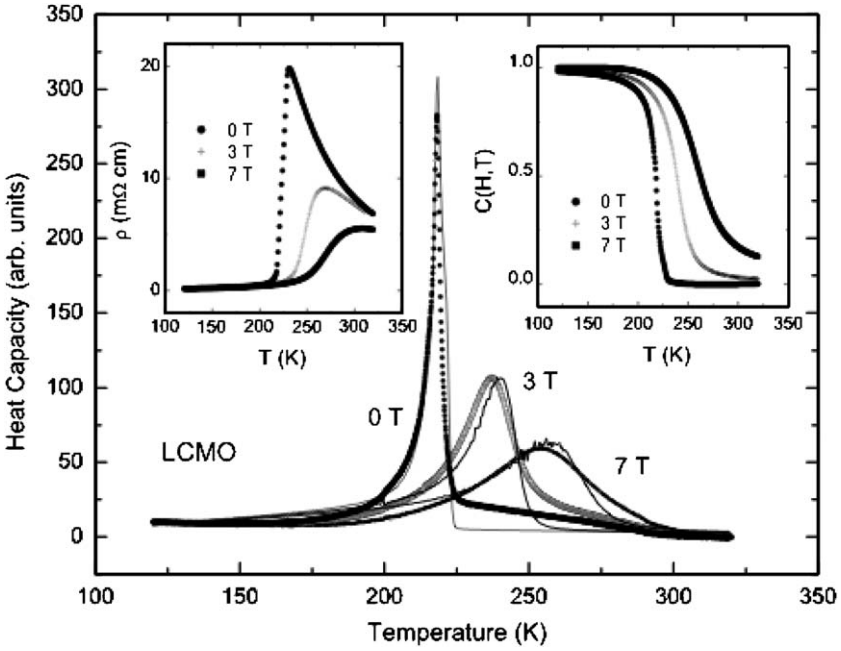

Fig. 21. Heat capacity as a function of field for $La_{0.67}Ca_{0.33}MnO_3$ and a calculation based on a two-state model. The insets show the resistivity and the metallic fraction $c(H)$ extracted using an effective medium approach. Taken from Ref. [179].

grow in number but not in size. This results in a sudden connection of clusters, leading to percolation—but of a very special sort. The Griffiths phase and nanoscopic phase separation is discussed by Burger et al. [181].

The Griffiths phase encompasses that range of temperatures between the maximum possible transition temperature T_G and the observed one at the Curie temperature T_C. The treatment of the Griffiths phase was extended by Bray [182] and is based on the Lee and Yang approach to phase transitions [183]. In this framework the partition function Z for a system undergoing a phase transition can be expressed as a polynomial with all positive terms that may be factored into N complex roots, where N is the number of particles in the system.

$$Z = e^{Nh} \prod_i (z - z_i) \tag{1}$$

and

$$\frac{F}{kT} = Nh + \sum_i (z - z_i), \tag{2}$$

where in both expressions $z = \exp(-2h)$, h is the scaled magnetic field and the product or sum is taken over the index i, where i runs from 1 to N. The theory of Lee and Yang states that all z_i lie on the unit circle in the complex plane and can be written as $z_i = \exp(i\theta_i)$, where θ_i provides a measure of the angle on the unit circle. The problem thus collapses into determining the distribution of zeroes on the unit circle. With that distribution given by $g(\theta)$, the magnetic susceptibility is

$$\chi = \frac{6C}{T} \int_0^{\pi} \frac{g(\theta, t)}{1 - \cos\theta} \, d\theta. \tag{3}$$

The magnetic susceptibility will diverge when there is a finite probability of a zero at $\theta = 0$. The essence of the Griffiths singularity is that there is a pile-up of zeros near, but not at, $\theta = 0$, followed by a sudden collapse of the distribution.

In this framework, many aspects of the system—the magnetic susceptibility, the rapid rise of the magnetization at T_c (upon cooling) and the small entropy associated with the transition—can be reproduced with particular forms for $g(\theta)$ [184]. Furthermore, the lower the value of T_c is, the less entropy change there is in the vicinity of the transition. The large number of Yang–Lee zeroes at small θ translates into a large number of regions with large susceptibility. This makes the effective spin large in the Griffiths phase, and releases much of the ordering entropy well above the transition. To the extent that the low temperature phases are suppressed by disorder, the region between the "pure" transition and the actual one may be indeed a Griffiths phase [185]. Hence, an interesting direction for high resolution magnetic scattering is to follow the development of these numerous, highly correlated magnetic regions and to study their evolution with magnetic field and temperature.

5.2. Inhomogeneity in complex magnetic systems

Inhomogeneities can be driven thermodynamically by chemical doping or competing interactions at the nanoscale, as is the case of CMR and high-T_c superconductors, or introduced via artificially tailored synthesis, as is the case of magnetic nanocomposites. Inhomogeneity can also be thought of as a self-assembly process driven by quantum fluctuations (at least for those systems sitting near quantum critical points or with nearly degenerate phases.) The existence of inhomogeneity in complex systems has been conclusively proven to exist experimentally in many systems [167,186] and this inhomogeneity can indeed be reproduced by phenomenological models [187]. Examples of this may be found in CMR materials, in which ferromagnetic metallic regions coexist with antiferromagnetic insulating regions at the nanoscale [188]. In high-T_c superconductors, nanoscale inhomogeneities in all electronic, magnetic and structural degrees of freedom have been observed [189,190]. Inhomogeneities exist by design in magnetic nanocomposites, such as in exchange-spring magnets [191–193] that consist of hard and soft magnetic phases mixed at the nanoscale in a quest to achieve improved permanent magnetic properties. Furthermore, inhomogeneities may also arise at interfaces from the complex interplay between the electronic structures of dissimilar materials [194].

The existence of nanoscale ferromagnetic clusters in many materials previously thought to be homogeneous is now without question. It is thus necessary to inquire about the origins of the effect. It is not clear if the phase transition is one of nucleation and growth (thermodynamically first-order) or, as in spinodal decomposition, fundamentally second-order. Open questions under study currently include the influence of temperature and field on the phase separation, and whether the phase separation is reversible. Importantly, what are the structural precursors responsible for the phase separation phenomenon, if any? These need not be gross chemical segregation, but could be far more subtle, as e.g. in the LSMO manganites CMR material, spatial inhomogeneities in the oxygen stoichiometry, valence, Mn–O bond length, or very short length scale variations in the La/Sr ratio even in a nominally randomly doped system. The challenge is to determine if phase-separation phenomena are merely pinned by, as opposed to due to, the inevitable inhomogeneity of dopant distribution in such materials. In this regard, one critical issue concerns the question of the length scale of the phase components of a multi-phase complex system. In some systems segregation occurs on nanoscopic scales, while in other systems micron-sized segregation occurs [195]. It is possible that one case originates from intrinsic magneto-electronic segregation, while the other is due to structural inhomogeneity.

Such questions naturally lead from identification of phenomena to their exploitation. For example, understanding the segregation mechanism in ferromagnetic

phase-separated materials may lead to the creation of novel phase morphologies. Exciting possibilities resulting from control over the phase separation include self-assembly of 3D magnetic matrices consisting of lamellar, gyroidal or cylindrical (filamentary) geometries. Such architectures are anticipated to have technological implications, for example in GMR superlattices and exchange bias-based devices.

It is becoming increasingly clear that the underpinnings of inhomogeneity, such as local defects and chemical disorder, remain essential components of the physics of many material systems of interest (from heavy fermions to manganites to ferromagnetic semiconductors). Fig. 22 shows the change in magnetization of the ferromagnetic semiconductor (Ga, Mn)As with annealing at low temperatures (250 °C) for relatively short time periods from 10 min to 24 h [196]. The considerable changes in the form of the magnetization curve, as well as in the Curie temperature, can be attributed to the important role of defects. The atomic viewpoint of heterogeneity is extended to include site-specificity, in addition to element-specificity. Such studies provide understanding of the effects of inequivalent atomic environments on magnetic properties. For example, CMR and high-T_c oxide materials, as well as intermetallic permanent magnet compounds $Nd_2Fe_{14}B$ and Sm_2Co_7, all possess inequivalent crystal sites. Examples of these inequivalent crystal sites are the Mn^{3+} and Mn^{4+} sites in the CMR manganites and the the Cu(1) and Cu(2) sites in the CuO_2 planes of the cuprate superconductors. There are two Nd sites in $Nd_2Fe_{14}B$ [197], (the 4f and 4g sites, in Wykcoff notation) that are recognized to control the anisotropy of the compound (Fig. 23). Techniques such as magnetic resonant X-ray diffraction using circularly polarized X-rays can separate the magnetic contributions of these inequivalent sites [198,199]. Selection of a scattering vector along the high-symmetry [110] direction in the tetragonal P42/mnm $Nd_2Fe_{14}B$ structure allows structure factor contributions to the scattering from either one of the the other Nd site to nearly vanish, Fig. 24. This feature enables the determination of the magnetic behavior of each Nd site to be determined independently.

In addition to atomic defects, inhomogeneity at the micrometer scale such as grain structure may play an important role. For example, complex oxides are so sensitive to stoichiometry and strain that surfaces can exhibit significantly altered properties from the bulk. For nanostructures exhibiting 3D confinement, surfaces can have a dominant effect. However, the surfaces of bulk oxides are not completely understood. Thus, understanding the role of surfaces in confined oxides has three aspects: (i) the need to develop a fundamental understanding of unconfined surfaces; (ii) the need to clearly distinguish between bulk and surface effects; and (iii) a means to measure the physical and electronic structure of nanoconfined oxides, including effects of strain.

An example of progress toward the first goal is the discovery in bilayer manganites of a non-ferromagnetic, insulating surface bilayer capping a fully spin-polarized ferromagnetic bilayer beneath. (Fig. 25) [200] Applying advanced X-ray magnetic scattering and circular dichroism techniques together with point-contact and scanning tunneling spectroscopy (STM) to $La_{2-2x}Sr_{1+2x}Mn_2O_7$, it was concluded that the outermost Mn–O bilayer alone is affected. This intrinsic nanoskin is an insulator with no long-range ferromagnetic order, while the subsequent bilayer displays the full, bulk, spin polarization up to nearly the bulk Curie temperature. The magnetic 'bulk' bilayers are expected to be metallic due to hopping between Mn^{+3} and Mn^{+4} ions by double exchange in this doped manganite, while tunneling data suggest that the surface bilayer is an insulator. The abrupt changes in only the topmost bilayer are likely due to the weak electronic and

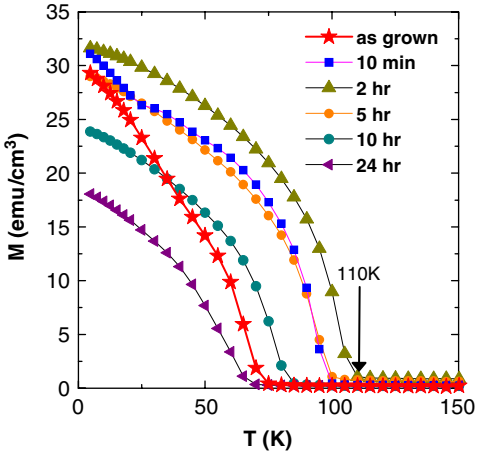

Fig. 22. Change in magnetization of (Ga,Mn)As with annealing at 250 °C for the specified time periods, taken from Ref. [196]. The changes in the magnetization and Curie temperature are attributed to the important role of defects, in particular the out-diffusion of Mn interstitials which are induced by the low temperature MBE growth required to make this material.

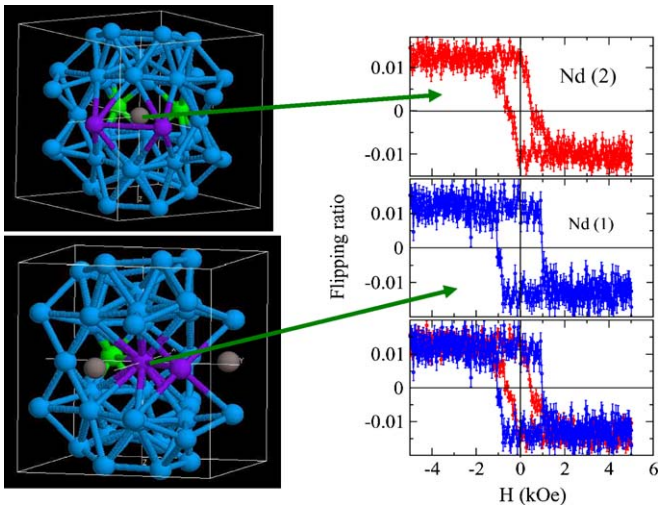

Fig. 23. Coexisting Nd crystalline environments in $Nd_2Fe_{14}B$ permanent magnet (left). Site-specific Nd hysteresis loops (right). The crystalline environment at the Nd(1) site results in its higher stability against demagnetizing fields. Based on Ref. [199], courtesy of D. Haskel.

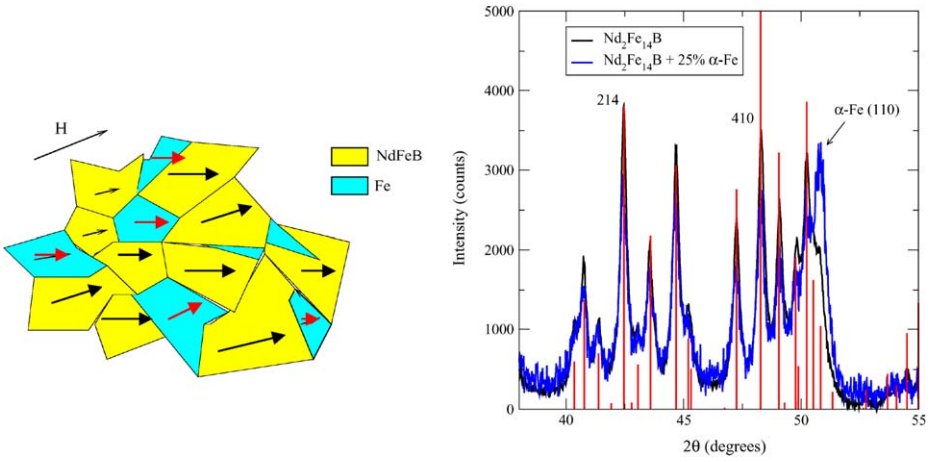

Fig. 24. Left: Schematic of exchange-coupled nanocomposite with hard and soft magnetic phases. Magnetic contributions from Fe atoms in either phase can be separated by selecting appropriate Bragg diffraction conditions (right) and using circularly polarized X-rays at Fe resonance to couple to their magnetic moments. Based on Ref. [199], courtesy of D. Haskel.

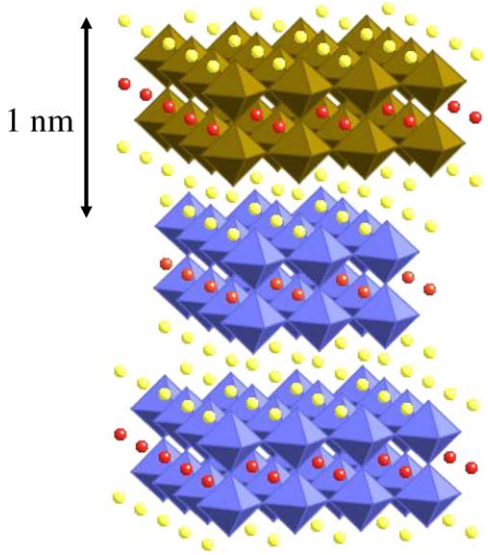

Fig. 25. Structure of the naturally bilayered manganite, $La_{2-2x}Sr_{1+2x}Mn_2O_7$. The MnO_6 octahedra denoted in blue and (La,Sr) sites shown as yellow and red dots. The bilayer repeat distance is ~10 Å. The non-ferromagnetic surface bilayer is colored brown [116].

magnetic coupling between bilayers engendered by the crystal structure.

The reason that the surface layer remains insulating in the layered manganite, above, is unclear. Surface sensitive spectroscopic measurements seem to exclude chemical disorder (loss of oxygen or cation segregation). One speculation is that the free surface promotes Mn^{+3}/Mn^{+4} ordering to better accommodate the strain of Jahn–Teller distortions of the Mn^{+3} ions. Another likely possibility is a reconstruction of the lattice in the surface bilayer, which would have a profound impact on the ground state of that layer. Surface-sensitive X-ray studies can provide a framework to understand how the electronic structure of the bulk is modified in the proximity of the surface. Concomitant scanning-tunneling spectroscopy (STS) will access low energy states closer to the Fermi level, but also may be exploited to connect the X-ray results to observations in confined nano-particles.

As another recent example related to the third goal above, it has recently been observed that more bulk sensitive hard X-ray photoemission at ~6 keV photon energy exhibits additional structure in Mn 2p core spectra from LSMO manganites that can be directly connected with doping-induced states [201]. Similar additional structure has been seen in high-energy photoemission from a variety of transition-metal oxides, including epitaxial thin films of LSMO, for which the presence/absence of these features can be directly correlated with the presence or absence of ferromagnetism induced by strain in the layers. Some of these results are summarized in Fig. 26 [202]. The ability to carry out photoemission measurements at energies up to about 10 keV thus provides an important new tool for studying magnetic materials and nanostructures, as amplified below.

5.3. *Multiferroic effects in complex systems*

Multiferroics are intriguing materials that exhibit strong coupling between various degrees of freedom: structural, electrical, magnetic and strain. Multiferroic materials are single-component materials or composites exhibiting two or more ferroic features such as ferromagnetism, ferroelectricity, or ferroelasticity/shape-memory effects [203,204]. While there are a number of materials that possess ferroic properties (i.e., ferromagnetism and ferroelasticity), there need not be a large coupling between the two properties. Hence multiferroics, by their very nature, are identified as complex materials. The number of single-phase materials with multiferroic potential is limited, and includes nickel iodine boracite [205] and mixed perovskites, notable Bi-based Fe- and Mn-perovskites [206,207]. Ni_2MnGa is a ferromagnetic ferroelastic Heusler alloy that may also be considered to be multiferroic [208]. An alternate materials

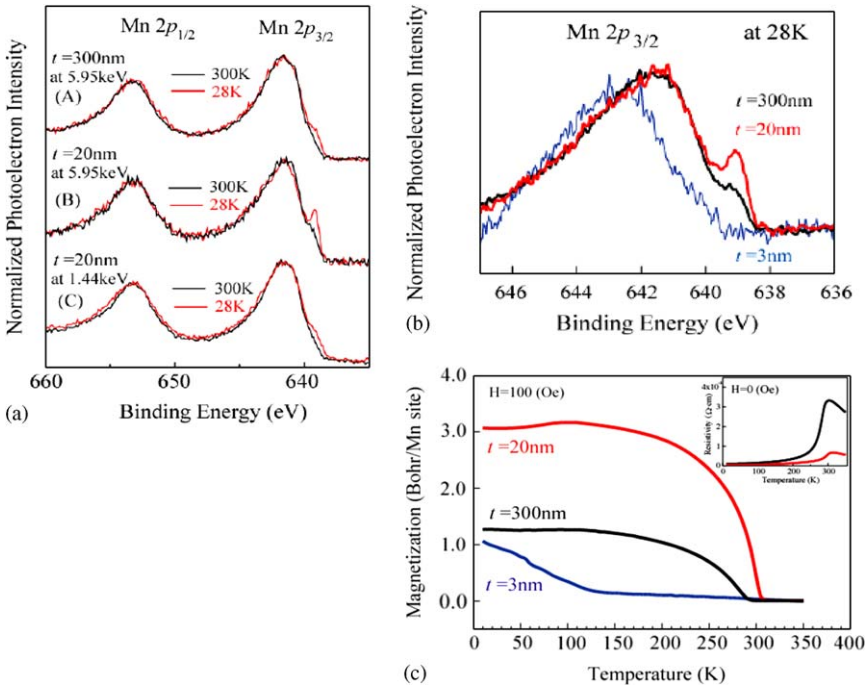

Fig. 26. (a) Mn 2p spectra from (La_0.85Ba0.15)MnO3 thin films, illustrating the additional feature at 639 eV binding energy observed only with more bulk sensitive 6 keV excitation. (b) The thickness dependence of this extra feature. (c) Measurements of magnetization M and resistivity ρ as a function of temperature, illustrating the correlation between them and the strength of the additional feature.

design strategy to obtain multiferroic behavior is to combine materials of two different functional characters (i.e. magnetoelectric, magnetostrictive) to create composites. Composite multiferroics have been produced over different length scales, from laminar geometries through nanoscale superlattices and self-organized structures [172,209]. In addition to the possibility of combining different ferroic effects, it is possible to tailor the multiferroic materials response via adjustment of the constituent volume fractions.

Recently, the hexagonal manganites ($RMnO_3$, with R = Er, Ho, In, Lu, Sc, Tm, Y, Yb) have aroused new interest as multiferroic materials [210]. This family of materials shows multiferroic behavior with a ferroelectric phase transition near ~900 K and an antiferromagnetic transition T_N~90 K, although the exact ordering temperatures and inherent interactions remain controversial [211]. In another multiferroic compound ($TbMn_2O_5$), a striking interplay between ferroelectricity and magnetism has been demonstrated where the electric polarization reversal and permanent polarization signature are both actuated by an applied magnetic field [212]. Many open questions surround multiferroic phenomena, including how the coupling between functional effects occurs.

6. Synchrotron X-ray techniques and relationship to nanomagnetism research

The application of synchrotron radiation to the study of magnetic materials has grown rapidly in recent years, owing in part to the availability of high-brightness synchrotron sources. Several characteristics of synchrotron radiation make the study of magnetic materials very attractive. First of all, the high brightness of the beam typically results in a flux of 10^{12-13} photons/s in less than a 1 mm^2 area, which enables the study of small or highly diluted samples. The high scattering wavevector resolution due to the X-ray collimation and monochromaticity permits precise determination of magnetic modulations. Furthermore, the well-defined polarization characteristics of synchrotron radiation (naturally linear in the plane of the storage ring, but also variable in polarization via specially designed undulators), together with its relatively simple manipulation and analysis by crystal optics, can be used to study a variety of magnetization states. Lastly, by tuning the energy of the incident beam near absorption edges (or resonances) of constituent elements, one can study the magnetic contributions of individual components in heterogeneous structures. Being able to vary photon energy over the approximate interval of 0.5–15.0 keV can also permit clearly distinguishing surface, interface, and bulk effects, as well as uncovering new effects that can be directly related to magnetism.

X-rays interact with matter by scattering from both the electron charge and its magnetic moment, as well as by being absorbed via electron excitation and the photoelectric effect. The charge scattering is the dominant term and is the basis for most condensed matter studies using X-rays. Although small, the scattering from the magnetic moment is sufficient to extract valuable information on

magnetic structures in single crystals [213–215]. Enhanced sensitivity to magnetic moments can be achieved by tuning the X-ray energy to selected resonances. These resonant enhancements have resulted in widespread applications of X-rays in the study of magnetism, both in the absorption (X-ray magnetic circular dichroism or XMCD) [216–218] and scattering (X-ray resonant magnetic scattering) [219,220] channels. These techniques include studies of interfacial magnetic roughness in multilayers [221–224], and of morphology of magnetic domains in buried interfaces [225,226]. Furthermore, by performing polarization analysis of the scattered radiation [227] or applying sum rules to dichroic absorption spectra of spin-orbit split absorption edges [228] it is possible to distinguish between spin and orbital contributions to the magnetic moment in an element-specific manner. This is a unique attribute of magnetic scattering and spectroscopy techniques, and it is the primary reason why these techniques are powerful tools in magnetism studies. Recent reviews of general applications of X-rays to study magnetism are given by Gibbs, Hill and Vettier [229] and by McWhan [230].

Most synchrotron studies of nanomagnetism to date have been performed using soft X-rays (loosely defined as possessing energy < 3 keV) since resonant dipolar transitions in this energy regime access electronic states carrying large magnetic moments in most materials (e.g., $2p \rightarrow 3d$ states in transition metals, and $4d \rightarrow 4f$ states in rare-earths.) Hence, the magnetic signals are larger and easier to observe. Harder X-ray energies (> 3 keV) access electronic states with smaller, yet significant, magnetic moments (e.g., $1s \rightarrow 4p$ states in transition metals and $2p \rightarrow 5d$ states in rare-earths). While experimentally more challenging, hard X-ray studies of magnetism offer unique advantages. The higher penetrating power of these X-rays enables the study of buried structures and interfaces, which can be important in characterizing a wide variety of magnetic systems used in modern technologies, such as permanent magnetic materials and artificial, thin-film heterostructures. The penetrating power of hard X-rays yields a true bulk-measurement probe without the need for high-vacuum conditions, while soft X-ray measurements are surface sensitive and must be performed in ultrahigh vacuum conditions. Furthermore, the shorter hard X-ray wavelengths permit diffraction studies to probe the magnetic order in both crystals and artificial, periodic nanostructures, such as multilayers and patterned dot/hole arrays.

The rich polarization dependence of magnetic scattering can be used to extract the magnetic ordering of a material. Antiferromagnetic (AF) structures are commonly studied with linearly polarized radiation. In the absorption channel, the linear magnetic dichroism (MLD) effect [231,232] results in absorption contrast for parallel and perpendicular alignments of the X-ray's linear polarization and the sample's magnetization in the presence of magneto-crystalline anisotropy, which can be used, e.g., to image AF domains in exchange-biased systems [233]. In the diffraction channel, AF ordering results in Bragg diffraction at the magnetic ordering's wavevector. As discussed below, synchrotron radiation brightness, together with resonant enhancement of the magnetic scattering cross section, can result in the detection of X-ray magnetic scattering from AF systems. Circularly polarized (CP) radiation can also be useful in studies of AF materials. CP X-rays were used for real-space imaging of chiral domains by helicity-dependent Bragg scattering from the spiral AF state of a Ho crystal by Lang et al. [234].

Ferri- or ferromagnetic structures are commonly studied with CP radiation. In the absorption channel, XMCD results in absorption contrast for parallel and antiparallel alignment of the X-ray helicity and the sample magnetization.216 By measuring this absorption contrast in spin-orbit split core levels (e.g., transition metal L_2 and L_3 edges), element-specific magnetic moments in the final state of the absorption process (both spin and orbital components) can be extracted by application of sum rules [235,236]. This contrast, in combination with focused X-ray beams, can be used to image ferromagnetic domains in nanostructures [237].

The pulsed nature of synchrotron sources offers the possibility of studying time-dependent phenomena. One of the desirable experimental capabilities is to achieve a high spatial resolution (~ 5 nm) and combine it with fast temporal resolution (~ 1 ps.) Neither of these capabilities are currently available at the APS. Time resolution depends on the electron bunch structure and, at the APS, the most common operating mode with 24 bunches equally distributed around the storage ring enables 153-ps time resolution. There is a considerable effort under way to reduce the time resolution to ~ 1 ps [238]. Pump–probe type experiments, schematically shown in Fig. 27, open new approaches to study the dynamics of magnetization reversal.

Selected examples will now be used to highlight the relationship of synchrotron-based X-ray techniques, both existing and under development, to address key scientific and technological issues associated with confined magnets. Then the complementarity of X-ray and neutron techniques are discussed, and the requirements for X-ray techniques and associated equipment developments in the future are outlined.

6.1. Buried solid–solid interfaces

Buried solid–solid interfaces are ubiquitous in nanomagnetic structures. Critical to the characterization process is a detailed understanding of their chemical concentration profiles, element-specific chemical states and magnetic properties, as well as quantitative chemical and magnetic roughness parameters. For example, X-ray standing waves in the 0.05–10 keV range can provide powerful methods for studying such interfaces. These standing waves can be created by Bragg reflection from any multilayer structure [239], or from any set of atomic planes in a single crystal or an epitaxial sample. Interfaces that exhibit lateral spatial

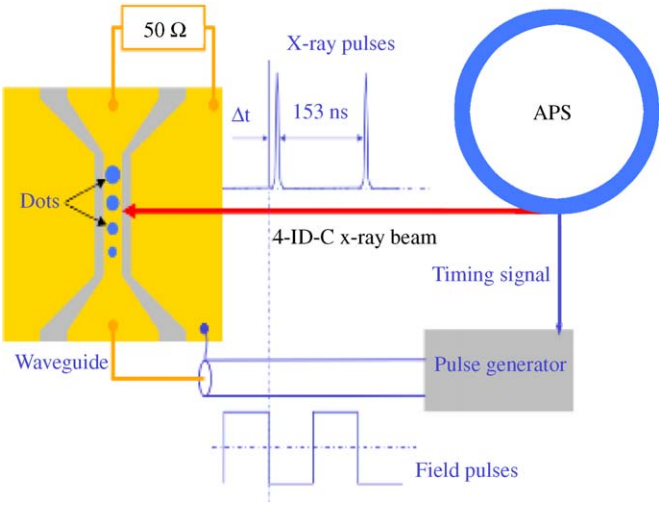

Fig. 27. Schematic of a typical pump–probe experiment at the APS. In this example, a current signal that creates a transient magnetic field is applied synchronously with the X-ray pulse in order to study magnetization dynamics in permalloy dots grown on top of a coplanar waveguide. For most of the time, the APS storage ring runs in a 24-bunch operating mode delivering X-ray pulses separated by 153 ns and lasting ~100 ps. In a 324-bunch special mode, the separation between X-ray pulses is 11.2 ns (courtesy D. Keavney).

variations, or wedge profiles, permit the standing wave to be scanned through the interface simply by moving a focused X-ray beam along the thickness gradient [240]. The experimental geometry and some results for such measurements are shown in Fig. 28. Such data can be obtained under both resonant and non-resonant conditions, and with either photoelectrons or fluorescent X-rays as the detection mode. For instance, measurements for an Fe/Cr interface with an excitation energy ~800 eV using, photoelectron detection yield the compositional variation of the buried interface, and via XMCD, the magnetization profile across the interface of Fe and Cr [240] Fig. 28 also shows some of the data obtained in this study, together with the concentration and magnetization profiles determined from it. Using even higher energies (5–10 keV range) would provide greater probing depths for both photoelectrons and X-rays, as well as stronger standing wave effects due to higher reflectivity [241]. With a focused X-ray beam, such measurements would also provide lateral microscopy information. The status of various types of standing wave experiments is discussed elsewhere [242]. The use of these techniques for studies of buried interfaces should provide solutions to many interesting and challenging problems in the field of nanomagnetism.

6.2. Resonant spectroscopies

Resonant spectroscopies of 3d TM films at the L edges provide various opportunities to investigate magnetic and chemical structure of magnetic matter at the nanometer scale [243]. In recent years emerging resonant small-angle scattering (SAS) techniques have been exploited to probe in-plane structural and magnetic order, over length scales ranging from the X-ray wavelength λ, 1–2 nm, up to ~300 nm [244–247] Magnetic and structural heterogeneities can be separated and quantified by tuning both the energy and polarization of the incoming X-ray radiation. For example, these techniques have been used to investigate the role of Cr in advanced magnetic recording medial alloys. The Cr is predominantly non-magnetic in CoPtCrB alloy media, thus, tuning the X-ray energies through the Cr edge enhances the chemical contrast, while tuning to the Co edge enhances both chemical and magnetic contrast.

6.3. Isotope effect

X-ray techniques can be element specific; however they normally do not distinguish between different isotopes. In contrast, neutron scattering is very sensitive to the specific isotopic composition. This strong isotope contrast can be used in the case of neutron scattering to enhance scattering contrast for magnetic structures by reducing the contrast for chemical structures [248]. However, X-ray techniques also become isotope-sensitive in the case of nuclear resonant scattering, which is related to the well-established Mössbauer effect. This technique is restricted to Mössbauer-active isotopes of elements such as Fe, Sn, Sm, Dy and Eu. Nuclear resonant scattering permits the measurement of nuclear hyperfine fields, which can be directly related to the magnetization vector [249]. Several key differences from the more traditional X-ray techniques (such as XMCD) are: (i) high spatial selectivity can be obtained by selective preparation of the sample with Mössbauer-active isotopes; (ii) the full direction of the magnetic moment in all three dimensions can be obtained; (iii) even for TM (such as Fe) the penetration depth is up to 100 nm, since hard X-rays can be used for the magnetic contrast (instead of soft X-rays at the L-edge); and (iv) they can be sensitive to atomic scale magnetic order, such as antiferromagnetism.

6.4. Complementarity of neutron and X-ray techniques

Since there are two major types of instruments that are relevant to address some of the issues outlined above, it may be worthwhile to highlight advantages and drawbacks of each. In the field of nanomagnetism, neutron scattering has several notable advantages, including the fact that it is a mature technique, it has substantial depth penetration, it is sensitive to isotopic substitutions, and the data interpretation is straightforward [250]. Its major disadvantage is low intensity and the necessity of large sample sizes to obtain data. Synchrotrons, however, provide high photon flux intensities (although this has to be normalized by the sensitivity to magnetism) and are element sensitive, but being relatively new, data interpretation is not necessarily direct [240]. Moreover, the high beam intensity can make sample heating a problem.

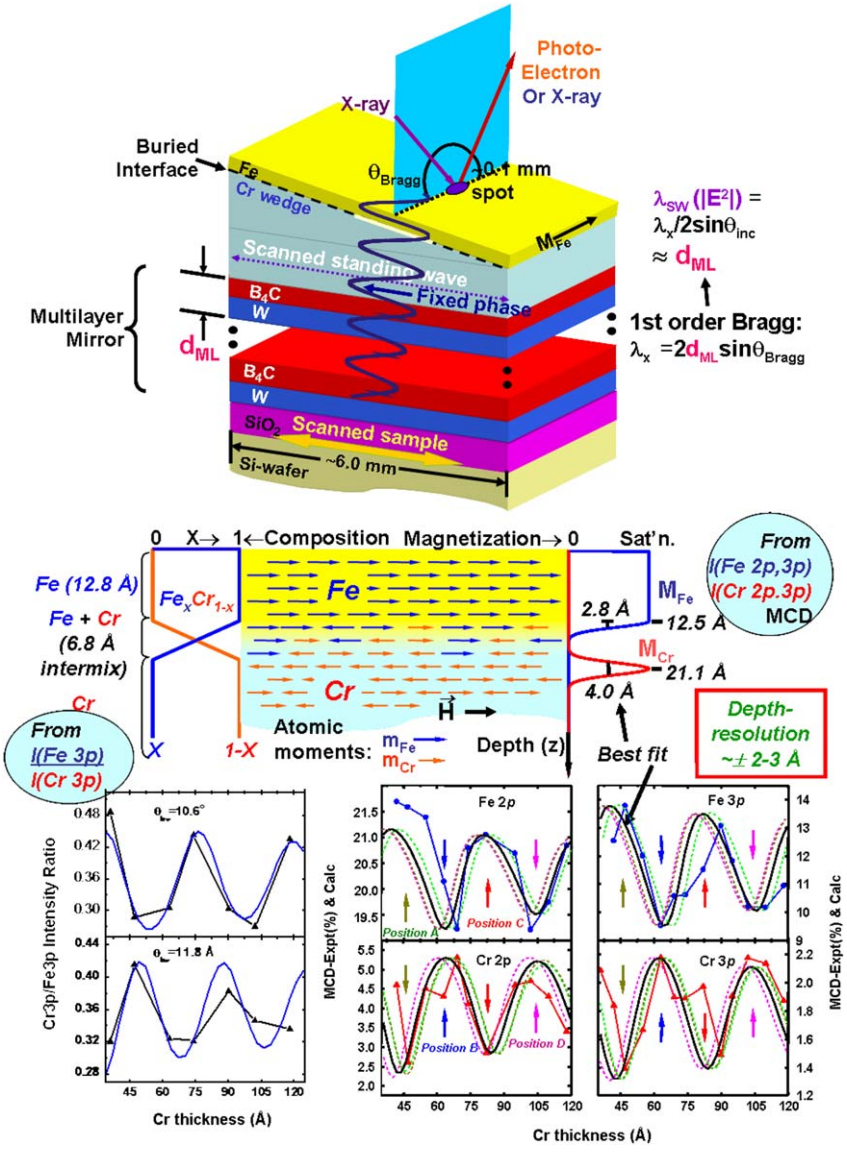

Fig. 28. Upper panel: schematic view of an experimental configuration permitting the selective excitation of photoelectrons or fluorescent X-rays from a multilayer magnetic system. Scanning the X-ray spot along the wedge permits scanning the standing wave through the Fe/Cr interface. Lower panel: intensity and magnetic circular dichroism results, together with X-ray optical theory permitting the derivation of the concentration and magnetization profiles shown.

An example of X-ray neutron complementarity appears in the recent work for Roy et al., on the depth profile of uncompensated spins in an exchange bias system [251]. Synchrotron sources have been built to optimize for either scattering or spectroscopy experiments. However, recent advances in synchrotron instrumentation have tended to blur this distinction so that advanced scattering experiments can often be performed at the lower-energy machines, while many low-energy spectroscopy techniques can be implemented at the higher-energy machines.

6.5. X-ray instrument requirements

A key experimental feature for most applications is the quality and versatility of the sample environment. As first priorities it is crucial to be able to cover a diverse parameter space that captures the novel properties of the multitude of systems of interest. This includes:

- Temperature range: 1–500 K.
- Magnetic fields up to 12–20 T.
- 3D Magnetic field orientation.
- Ultra-low remanent field.
- Pressure range to include that available via diamond-anvil cell techniques.
- Optical, electrical access.

Beyond these needs, of course, it would be useful to have ultra-low temperatures <1 K and very high fields >20 T for select applications. Additionally, in situ sample

preparation is of high priority in many experiments, especially for surface magnetism experiments. The APS can already offer a subset of choices from the menu above, such as a temperature range from 6–500 K and magnetic fields up to 4 T. Presently, there is a strong emphasis on the development of high-pressure capabilities up to 20 GPa via diamond-anvil cells in a magnetic field up to 1 T. In addition, plans are underway to introduce in situ transport and optical measurements in combination with X-ray techniques. Also, there are near-term plans to offer the scientific community access to high field capabilities up to 13 T. In the context of a synchrotron facility, effective implementation and efficient operation of most of these specialized instruments require either dedicated beamlines or dedicated end-stations. Since it is unrealistic to pursue parallel development of all new capabilities, the input of the nanomagnetism community will continue to be crucial in setting the proper priorities so that hard X-ray scattering, spectroscopy and microscopy techniques will remain indispensable tools in nanomagnetism studies well into the 21st century.

Medium and hard X-ray spectroscopies, applied with dichroism and spin resolution, as well as spatial and time resolution, should be key elements of the APS 10-year plan. Absorption and scattering will clearly be a part of this, as one of the standard hard-X-ray experiments, but it should be stressed that developing world-class facilities for photoemission, such as described in the next subsection, if possible, coupled with soft and/or hard X-ray emission/absorption in the same chamber would also be extremely valuable.

6.6. Specific examples of desirable capabilities

6.6.1. Hard X-ray photoemission

High-energy photoemission/diffraction/microscopy in the 5–10 keV range would be desirable: Photoemission is one of the most powerful spectroscopic tools in synchrotron radiation science, but at the excitation energies of 20–1500 eV typically used today, it is a mixed surface and bulk probe, with electron inelastic attenuation lengths in the 0.5–2 nm range. Exciting photoelectrons in the 5–10 keV range would provide enhanced bulk sensitivity, which could be varied via decreased takeoff angle. This advance would reduce sample transfer and preparation problems as well as permit the measurement of properties that are more truly representative of bulk behavior well below the surface, as discussed in a prior section [201]. The fact that bulk-associated spectral features are seen in hard X-ray photoemission that do not appear in soft X-ray photoemission [202] also points out that we cannot hope to fully understand electronic and magnetic structure in complex systems without making measurements in both regimes of energy. In this regard, overall instrumental resolutions of about 50 meV have already been reported [252]. Such an experimental system should be mated to a variable polarization undulator with XMCD/MLD capabilities and a finely-focussed X-ray beam; the APS is planning such a beamline that will go to 50 nm. Additional capabilities would permit measuring element-specific electronic structure, magnetic spin and orbital moments, and valence-level densities of states, all with spin resolution. One recent example of the power of applying core level and valence band spectroscopies to magnetism is found in studies of the CMR oxide LSMO [253] carried out in the soft X-ray regime. In this study, a dramatic change in the Mn magnetic moment was observed through a Mn 3 s multiplet splitting, and via concomitant O 1 s binding energy shifts and other core and valence spectral changes, it was deduced that a high-temperature high-spin phase associated with Jahn–Teller distortion and polaron formation was present [253]. Most of the data obtained in this study could have been obtained with hard X-rays, thus reducing the questions of surface vs. bulk effects that complicated data analysis. Taken together with work such as shown in Fig. 26 [202] and that in Ref. [201], these results make it clear that hard X-ray photoemission of core and valence levels will make an important contribution to future studies in nanomagnetism. Extending beyond this capability, atomic structural information, again element-specific, may be obtained from photoelectron diffraction and holography [254]. Furthermore, spin-polarized photoelectron diffraction and holography would permit determining local magnetic order in complex materials [255,256].

6.6.2. Standing wave studies

Standing wave studies of buried interfaces in the 0.5–10 keV range is another desirable capability. Although many powerful tools for studying solid–vacuum interfaces currently exist (e.g. LEED, STM, AFM, photoemission, surface X-ray diffraction), none of these tools permits a direct probe of the buried solid–solid interfaces that are ubiquitous in nanomaterials. One very promising method for selectively probing such buried interfaces is to use an X-ray standing wave for exciting photoelectrons or fluorescent X-rays, with the excitation strength modulated by a roughly $\sin^2 z$ variation that may penetrate through the interface [257]. Strong standing waves are thus created either by diffraction from suitable crystal planes (*e.g.* in the layered manganites [258]) or from an artificial multilayer structure [259]. Detecting both photoelectrons and fluorescent X-rays would provide greater/lesser degrees of bulk sensitivity, as well as complementary information on electronic and magnetic structure. Furthermore, a combination of standing-wave excitation techniques with lateral spectromicroscopy would provide truly 3D microscopy [257].

6.6.3. Holographic opportunities

X-ray *fluorescence holography—sub-Å imaging with no phase problem* represents another fruitful frontier. This experiment provides elementspecific local 3D atomic structure in two ways: (i) with a fixed exciting-beam

direction by measuring the angular distribution of outgoing fluorescent X-rays as the hologram [260]; or (ii) by carrying out the same experiment in a time-reversed mode, in which the direction of the exciting beam is varied with respect to crystal axes, and the intensity of a given atom's fluorescent X-rays is monitored to yield the hologram [261]. A simple Fourier-transform type of inversion algorithm, most powerful in a multi-energy mode then yields the atomic images. Various demonstration experiments of this type have been performed, and future possibilities for enhancing image accuracy and dimensions (including magnetic structure) have recently been reviewed [262,263]. Beyond prior studies, which have demonstrated the element-specific structural capability at the ~0.1 Å level, and have imaged about 40 near-neighbor atoms around a given center atom [264], a recent theoretical study suggests that, by going on- and off-resonant scattering conditions for a given element, and then analyzing suitable differences of non-resonant and resonant holograms, the elemental identity of the near-neighbor atoms may be determined [265], with one experimental study recently seeming to verify this prediction [266]. No other structural probe permits the uniquely identification of the neighbors of a given type of atom.

6.6.4. *Advanced detector development*

Supplemental technological activities that will enable the application of these advanced synchrotron techniques include the development of next-generation, pixilated, IC-based detection systems for both X-rays and electrons. For example, a 1D detector for electrons that has been developed at the Advanced Light Source in Berkeley, could increase count rates by factors of 10^2–10^3, permitting time-resolved pump–probe studies in the ~200 μs timescale [267,268]. Beyond this, a large-surface, pixilated, energy-resolving X-ray detector would permit time-resolved EXAFS, as well as make X-ray holography a more accessible and more widely utilizable technique. Finally, research and development is needed for a more efficient next-generation approach for electron spin detection, for example, via exchange scattering or spin filtering through a ferromagnetic thin film. Nanomagnetism research carried out with synchrotron radiation would be enormously enhanced by such a spin detector, even if it only increased efficiencies by a factor of 10.

7. Brief summary

This report attempts to accomplish a number of goals. One is to provide a contemporary glimpse of the field of nanomagnetism. The perspective is necessarily that of the authors. The field is diverse enough that a different collection of authors might frame the picture somewhat differently, but hopefully much of the major interest is included here. We have divided the field into three thematic areas based on three interesting types of materials: patterned nanostructures, clusters, and complex oxides. Another goal was to look into the future and identify the grand challenges that lie ahead. Of course, such lists of challenges evolve with time as breakthroughs in our understanding emerge. Often the most interesting questions get addressed by parsing them into a different set of questions. As scientists we often answer questions by posing new questions. Having identified where we have been as a field, and where we think we are heading, enables us to plan for the research and instrumentation requirements needed to address the challenges and to probe the difficult questions in the field. This takes the report full circle, because the workshop that served to launch the present report focused on the future needs for hard X-ray synchrotron light sources. While it is hoped that the present report has value beyond this limited goal, such planning is important in its own right. This is because synchrotron light sources, and major facilities for materials research in general, occupy a significant part of the materials-research funding portfolio. As such, the report makes a number of recommendations to extend the temperature, pressure, and magnetic field characteristics that are accessible at synchrotron beamlines. It also specifically addresses several new techniques and instrumentation directions that are crucial to the next generation of experiments. There is also a desire to have simultaneous access to enhanced optical and electrical support systems within the sample environment. These generic requirements will enhance a range of experiments that exploit the spatial, temporal, and materials realms that can be explored.

Acknowledgements

We thank the following workshop participants: G. Aeppli, K. Attenkofer, C.-L. Chien, P. Crowell, E. Dagotto, J. Freeland, M. Freeman, K. Gray, D. Haskel, D. Keavney, C. L'abbé, J. Lang, D. Lederman, C. Leighton, H. Ohldag, S. Park, T. Rahman, T. F. Rosenbaum, M. Sarachik, P. Schiffer, and J. Slaughter. We also deeply appreciate the support provided by Suzanne Marik in preparing this paper.

Work was supported by the US DOE-BES at ANL under Contract no.W-31-109-ENG-38, at BNL under Contract no. DE-AC02-98CH10886, at LBNL under Contract no. DE-AC03-76SF00098, at ORNL under Contract no. DE-AC05-00OR22725, at UIUC under Award no. DEFG02-91ER45439 through the Frederick Seitz MRL and the CMM, and at UCSD under Contract no. FG03-87ER-45332. Work at UW was supported by NSF grants DMR-0203069 and DMR-0501421 and the Campbell Endowment. Work at CMU was supported by NSF grants CTS-0227645 and ECS-0304453. Work at KSU was partially supported from a grant from DOE (DE-FG02-03ER46058) and another from NSF (NER0304665). Work at MIT was supported through NSF MRSEC DMR 0213282 and ECS 0322027.Work at OSU was supported by DOE Grant Nos. DE-FG02-86ER45271 and DE-FG02-01ER45931.

References

[1] S.D. Bader, Rev. Mod. Phys. 78 (2006) 1.
[2] A. J. Freeman, S. D. Bader, (Eds.), Magnetism Beyond 2000, J. Magn. Magn. Mater. 200, 1999.
[3] J. Martin, J. Nogues, K. Liu, J.L. Vicent, I.K. Schuller, J. Magn. Magn. Mater. 256 (2003) 449.
[4] I.K. Schuller, S. Kim, C. Leighton, J. Magn. Magn. Mater. 200 (1999) 571.
[5] G.A. Prinz, Phys. Today 48 (1995) 58.
[6] I. Zutíc, J. Fabian, S. Das Sarma, Rev. Mod. Phys. 76 (2004) 323.
[7] M.N. Baibich, J.M. Broto, A. Fert, F. Nguyen Van Dau, F. Petroff, P. Eitenne, G. Creuzet, A. Friederich, J. Chazelas, Phys. Rev. Lett. 61 (1988) 2472.
[8] I.K. Schuller, C.M. Falco, J. Hilliard, J. Ketterson, B. Thaler, R. Lacoe, R. Dee, in modulated structures-1979, AIP Conf. Proc. 53 (1979) 417.
[9] P. Grünberg, US Patent # 4,949,039, 1990.
[10] J.A. Katine, F.J. Albert, R.A. Buhrman, E.B. Myers, D.C. Ralph, Phys. Rev. Lett. 84 (2000) 3149.
[11] M. Johnson, R.H. Silsbee, Phys. Rev. Lett. 94 (2005) 047204.
[12] F.J. Jedema, A.T. Filip, B.J. van Wees, Nature (London) 410 (2001) 345.
[13] Y. Ji, A. Hoffmann, J.S. Jiang, S.D. Bader, Appl. Phys. Lett. 85 (2004) 6218.
[14] S.A. Crooker, M. Furis, X. Lou, C. Adelmann, D.L. Smith, C.J. Palmstrøm, P.A. Crowell, Science 309 (2005) 219.
[15] J.E. Hirsch, Phys. Rev. Lett. 83 (1999) 1834.
[16] M. Hehn, K. Ounadjela, J.-P. Bucher, F. Rousseaux, D. Decanini, B. Bartenlian, C. Chappert, Science 272 (1996) 1782.
[17] C.A. Ross, Annu. Rev. Mater. Res. 31 (2001) 203.
[18] J.G. Zhu, Y. Zheng, G.A. Prinz, J. Appl. Phys. 87 (2000) 6668.
[19] L.J. Heyderman, C. David, M. Kläui, C.A.F. Vaz, J.A.C. Bland, J. Appl. Phys. 93 (2003) 10011.
[20] S. Kasai, E. Saitoh, H. Miyajima, J. Appl. Phys. 93 (2003) 8427.
[21] R.P. Cowburn, A.O. Adeyeye, M.E. Welland, Phys. Rev. Lett. 81 (1998) 5414.
[22] K.J. Kirk, J.N. Chapman, S. McVitie, P.R. Aitchison, C.D.W. Wilkinson, Appl. Phys. Lett. 75 (1999) 3683.
[23] R.P. Cowburn, D.K. Koltsov, A.O. Adeyeye, M.E. Welland, D.M. Tricker, Phys. Rev. Lett. 83 (1999) 1042.
[24] T. Shinjo, T. Okuno, R. Hassdorf, K. Shigeto, T. Ono, Science 289 (2000) 930.
[25] J.G. Zhu, Y. Zheng (Eds.), Spin Dynamics in Confined Magnetic Structures, 2002 p. 289.
[26] J. Bekaert, D. Buntinx, C. Van Haesendonck, V.V. Moshchalkov, J. De Boeck, G. Borghs, V. Metlushko, Appl. Phys. Lett. 81 (2002) 3413.
[27] U. Welp, V.K. Vlasko-Vlasov, G.W. Crabtree, J. Hiller, N. Zaluzic, V. Metlushko, B. Ilic, J. Appl. Phys. 93 (2003) 7056.
[28] J. Rothman, M. Kläui, L. Lopez-Diaz, C.A.F. Vaz, A. Bleloch, J.A.C. Bland, Z. Cui, R. Speaks, Phys. Rev. Lett. 86 (2001) 1098.
[29] F.J. Castaño, C.A. Ross, C. Frandsen, A. Eilez, D. Gil, H.I. Smith, M. Redjdal, F.B. Humphrey, Phys. Rev. B 67 (2003) 184425.
[30] L.J. Heyderman, C. David, M. Klaui, C.A.F. Vaz. J.A.C. Bland,, J. Appl. Phys. 93 (2003) 10011.
[31] F.J. Castaño, D. Morecroft, W. Jung, C.A. Ross, Phys. Rev. Lett. 95 (2005) 137201.
[32] F.Q. Zhu, D. Fan, X. Zhu, J.-G. Zhu, R.C. Cammarata, C.L. Chien, Adv. Mater. 16 (2004) 2155.
[33] M. Tsoi, J.Z. Sun, M.J. Rooks, R.H. Koch, S.S.P. Parkin, Phys. Rev. B 69 (2004) 100406(R).
[34] S.I. Kiselev, J.C. Sankey, I.N. Krivorotov, N.C. Emley, R.J. Schoelkopf, R.A. Buhrman, D.C. Ralph, Nature (London) 425 (2003) 380.
[35] Y. Huai, M. Pakala, Z. Diao, Y. Ding, IEEE Trans. Mag. 41 (2005) 2621 Oct.
[36] E.D. Daniel, C.D. Mee, M.H. Clark (Eds.), Magnetic Recording: The First 100 Years, IEEE Press, New York, 1998.
[37] L. Néel, Compt. Rend. Acad. Sci. 228 (1949) 664.
[38] A. Moser, K. Takano, D.T. Margulies, M. Albrecht, Y. Sonobe, Y. Ikeda, S. Sun, E.E. Fullerton, J. Phys. D: Appl. Phys. 35 (2002) R157.
[39] E.E. Fullerton, D.T. Margulies, M.E. Schabes, M. Carey, B. Gurney, A. Moser, M. Best, G. Zeltzer, K. Rubin, H. Rosen, Appl. Phys. Lett. 77 (2000) 3806.
[40] H. Do, E. E. Fullerton, D. T. Margulies, H. Rosen, US Patent # 6,372,330.
[41] K. Tang, C. Tsang, M. Mirzamaani, M. Doerner, A. Polcy, X. Bian, D.T. Margulies, E.E. Fullerton, L. Tang, N. Supper, M. Mercado, IEEE Trans. Mag. 40 (2004) 3548.
[42] D.T. Margulies, M.E. Schabes, N. Supper, H. Do, A. Berger, A. Moser, P.M. Rice, P. Arnett, M. Madison, B. Lengsfield, H. Rosen, E.E. Fullerton, Appl. Phys. Lett. 85 (2004) 6200.
[43] A. Moser, C. Bonhote, Q. Dai, H. Do, B. Knigge, Y. Ikeda, Q. Le, B. Lengsfield, S. MacDonald, J. Li, V. Nayak, R. Payne, M. Schabes, N. Smith, K. Takano, C. Tsang, P. van der Heijden, W. Weresin, M. Williams, M. Xia, J. Magn. Magn. Mater. 2006, in press.
[44] S.B. Darling, S.D. Bader, J. Mater. Chem. 15 (2005) 4189.
[45] K. Liu, S.M. Baker, T.P. Russell, I.K. Schuller, Phys. Rev. B 63 (2001) 060403.
[46] F.S. Bates, G.H. Fredrickson, Phys. Today 52 (2) (1999) 32.
[47] M. Park, C. Harrison, P.M. Chaikin, R.A. Register, D.H. Adamson, Science 276 (1997) 1401.
[48] T. Thurn-Albrecht, J. Schotter, C.A. Kastle, N. Emley, T. Shibauchi, L. Krusin-Elbaum, K. Guarini, C.T. Black, M.T. Tuominen, T.P. Russell, Science 290 (2000) 2126.
[49] J.Y. Cheng, W. Jung, C.A. Ross, Phys. Rev. B 70 (2004) 064417.
[50] M. Bal, A. Ursache, M.T. Tuominen, J.T. Goldbach, T.P. Russell, Appl. Phys. Lett. 81 (2002) 3479.
[51] J.Y. Cheng, A.M. Mayes, C.A. Ross, Nature Mater. 3 (2004) 823.
[52] K. Naito, H. Hieda, M. Sakurai, Y. Kamata, K. Asakawa, IEEE Trans. Magn. 38 (2002) 1949.
[53] S. Tehrani, J.M. Slaughter, M. Deherrera, B.N. Engel, N.D. Rizzo, J. Salter, M. Durlam, R.W. Dave, J. Janesky, B. Butcher, K. Smith, G. Grykewich, Proc. IEEE 91 (2003) 703.
[54] J.C. Slonczewski, Phys. Rev. B 39 (1989) 6995.
[55] J.C. Slonczewski, J. Magn. Magn. Mater. 159 (1996) L1.
[56] M. Tsoi, A.G.M. Jansen, J. Bass, W.-C. Chiang, M. Seck, V. Tsoi, P. Wyder, Phys. Rev. Lett. 80 (1998) 4281.
[57] J.Z. Sun, J. Magn. Magn. Mater. 202 (1999) 157.
[58] J.A. Katine, F.J. Albert, R.A. Buhrman, E.B. Myers, D.C. Ralph, Phys. Rev. Lett. 84 (2000) 3149.
[59] J. Z. Sun, IBM J. Res. Dev. 50 (2006) 81. 〈http://www.research.-ibm.com/journal/rd50-1.html〉.
[60] J.Z. Sun, Phys. Rev. B 62 (2000) 570.
[61] J.C. Kiselev, I.N. Sankey, N.C. Krivorotov, R.J. Emley, R.A. Schoelkopf, D.C. Buhrman, Ralph, Nature 425 (2003) 380.
[62] I.N. Krivorotov, N.C. Emley, J.C. Sankey, S.I. Kiselev, D.C. Ralph, R.A. Burhman, Science 307 (2005) 228.
[63] W.H. Rippard, M.R. Pufall, S. Kaka, S.E. Russek, T.J. Silva, Phys. Rev. Lett. 92 (2004) 027201.
[64] M.A. Hoefer, M.J. Ablowitz, B. Ilan, M.R. Pufall, T.J. Silva, Phys. Rev. Lett. 95 (2005) 267206.
[65] J.C. Slonczewski, J. Magn. Magn. Mater. 195 (1999) L261.
[66] M.L. Polianski, P.W. Brouwer, Phys. Rev. Lett. 92 (2004) 026602.
[67] B. Özyilma, A.D. Kent, J.Z. Sun, M.J. Rooks, R.H. Koch, Phys. Rev. Lett. 93 (2004) 176604.
[68] Y. Tserkovnyak, A. Brataas, G.E.W. Bauer, Phys. Rev. Lett. 88 (2002) 117601.
[69] R.H. Koch, J.A. Katine, J.Z. Sun, Phys. Rev. Lett. 92 (2004) 088302.
[70] J.Z. Sun, J.A. Katine, R.H. Koch, Proc. SPIE 5359 (2004) 445.

[71] A. Brataas, Y. Tserkovnyak, G.E.W. Bauer, B.I. Halperin, Phys. Rev. B 66 (2002) 060404.
[72] Y. Tserkovnyak, A. Brataas, G.E.W. Bauer, Phys. Rev. B 67 (2003) 140404(R).
[73] K. Xia, P.J. Kelly, G.E.W. Bauer, A. Brataas, I. Turek, Phys. Rev. B 65 (2002) 220401(R).
[74] Y. Tserkovnyak, A. Brataas, G.E.W. Bauer, B.I. Halperin, Rev. Mod Phys. 77 (2005) 1375.
[75] K.-J. Lee, A. Deac, O. Redon, J.-P. Nozières, B. Dieny, Nat. Mat. 3 (2004) 877.
[76] W.H. Rippard, M.R. Pufall, S. Kaka, S.E. Russek, T.J. Silva, Phys. Rev. Lett. 92 (2004) 027201.
[77] V. Synogatch, N. Smith, J.R. Childress, J. Appl. Phys. 93 (2003) 8570.
[78] M. Yamanouchi, D. Chiba, F. Matsukura, H. Ohno, Nature 428 (2004) 539–542.
[79] G. Tatara, H. Kohno, Phys. Rev. Lett. 92 (2004) 086601.
[80] M. Tsoi, R.E. Fontana, S.S.P. Parkin, Appl. Phys. Lett. 83 (2003) 2617–2619.
[81] J.A.H. Stotz, M.R. Freeman, Rev. Sci. Instr. 68 (1997) 4468.
[82] S. Kaka, S.E. Russek, App. Phys. Lett. 80 (2002) 2958.
[83] B.C. Choi, M. Belov, W.K. Hiebert, G.E. Ballentine, M.R. Freeman, Phys. Rev. Lett. 86 (2001) 728.
[84] C. Thirion, W. Wernsdorfer, D. Mailly, Nature Mat. 2 (2003) 524.
[85] J. Jorzick, S.O. Demokritov, B. Hillebrands, M. Bailleul, C. Fermon, K.Y. Guslienko, A.N. Slavin, D.V. Berkov, N.L. Gorn, Phys. Rev. Lett. 88 (2002) 047204.
[86] J.P. Park, P. Eames, D.M. Engebretson, J. Berezovsky, P.A. Crowell, Phys. Rev. Lett. 89 (2002) 277201.
[87] K.Y. Guslienko, B.A. Ivanov, V. Novosad, Y. Otani, H. Shima, K. Fukamichi, J. Appl. Phys. 91 (2002) 9037.
[88] J.P. Park, P. Eames, D.M. Engebretson, J. Berezovsky, P.A. Crowell, Phys. Rev. B 67 (2003) 020403R.
[89] S.B. Choe, Y. Acremann, A. Scholl, A. Bauer, A. Dornan, J. Stöhr, H.A. Padmore, Science 304 (2004) 420.
[90] J.P. Park, P.A. Crowell, Phys. Rev. Lett. 95 (2005) 167201.
[91] C. Bayer, J.P. Park, H. Wang, M. Yan, C.E. Campbell, P.A. Crowell, Phys. Rev. B 69 (2004) 134401.
[92] M.R. Freeman, B.C. Choi, Science 294 (2001) 1484.
[93] B.C. Choi, M. Belov, W.K. Hiebert, G.E. Ballentine, M.R. Freeman, Phys. Rev. Lett. 86 (2001) 728.
[94] H. Kachkachi, J. Mol. Liq. 114 (2004) 113–130.
[95] M.A. Nielsen, I.L. Chuang, Quantum Computation and Quantum Information, Cambridge University Press, Cambridge, 2004.
[96] S.T. Bramwell, M.J.P. Gingras, Science 294 (2001) 1495.
[97] E. Kneller, Fine Particle Theory, in: A.E. Berkowitz, E. Kneller (Eds.), Magn. Metall., New York, Academic, 1969 Ch. VIII.
[98] X. Batlle, A. Labarta, J. Phys. D: Appl. Phys. 35 (2002) R15.
[99] D. Luneau, Curr. Opin. Solid State Mater. Sci. 5 (2001) 123.
[100] I. Mirebeau, M. Hennion, H. Casalta, H. Andres, H.U. Güdel, A.V. Irodova, A. Caneschi, Phys. Rev. Lett. 83 (1999) 628.
[101] K.M. Mertes, Y. Suzuki, M.P. Sarachik, Y. Myasoedov, H. Shrikman, E. Zeldov, E.M. Rumberger, D.N. Hendrickson, G. Christou, Solid. State. Commun. 127 (2003) 131.
[102] J.R. Friedman, M.P. Sarachik, J. Tejada, R. Ziolo, Phys. Rev. Lett. 76 (1996) 3830.
[103] W. Wernsdorfer, R. Sessoli, Science 284 (1999) 133.
[104] Y. Shapira, M.T. Liu, S. Foner, R.J. Howard, W.H. Amstrong, Phys. Rev. B 63 (2001) 094422.
[105] S. Stolbov, R. A. Klemm, T. S. Rahman, First-Principles Calculations of the Magnetism of $Fe_2O_2H_2$, submitted; also available at 〈 http://arxiv.org/abs/cond-mat/0501178 〉.
[106] S. J. Etzkorn, J. Yang, L. Li, L. Dai, A. J. Epstein, submitted.
[107] D. Farrell, S.A. Majetich, J.P. Wilcoxon, J. Phys. Chem. B 107 (2003) 11022.
[108] D. Farrell, Y. Cheng, S. Kan, M. Sachan, Y. Ding, S.A. Majetich, L. Yang, J. Phys.: Conf. Ser. 17 (2005) 185.
[109] B.A. Korgel, D. Fitzmaurice, Phys. Rev. B 59 (1999) 14191.
[110] A.S. Dimitrov, K. Nagayama, Langmuir 12 (1996) 1303.
[111] M. Giersig, P. Mulvaney, J. Phys. Chem. 97 (1993) 6334.
[112] D. Farrell, Y. Ding, S.A. Majetich, C. Sanchez-Hanke, C.C. Kao, J. Appl. Phys. 95 (2004) 6636.
[113] D. Farrell, Y. Cheng, Y. Ding, S. Yamamuro, C. Sanchez-Hanke, C.-C. Kao, S.A. Majetich, J. Magn. Magn. Mater. 282 (2004) 1.
[114] S. Yamamuro, D. Farrell, S.A. Majetich, Phys. Rev. B 65 (2002) 224431.
[115] J.B. Kortright, O. Helwig, K. Chesnel, S. Sun, E.E. Fullerton, Phys Rev. B 71 (2005) 012402.
[116] J. Nogues, I.K. Schuller, J. Magn. Magn. Mater. 192 (1999) 203.
[117] A.E. Berkowitz, K. Takano, J. Magn. Magn. Mater. 200 (1999) 552.
[118] J. Nogués, J. Sort, V. Langlais, V. Skumryev, S. Suriñach, J.S. Muñoz, M.D. Baró, Phys. Rep. 422 (2005) 65.
[119] R.H. Kodama, A.E. Berkowitz, E.J. McNiff Jr., S. Foner, Phys. Rev. Lett. 77 (1996) 394.
[120] R.H. Kodama, J. Magn. Magn. Mater. 200 (1999) 359.
[121] W. Kohn, Rev. Mod. Phys. 71 (1999) 1253.
[122] W. Kohn, L. Sham, Phys. Rev. A 140 (1965) 1133.
[123] P. Hohenberg, W. Kohn, Phys. Rev. B 136 (1964) 864.
[124] J. Kübler, Theory of Itinerant Electron Magnetism Series: International Series of Monographs on Physics, Oxford University Press, New York, 2000.
[125] J.B. Staunton, B.L. Gyorffy, Phys. Rev. Lett. 69 (1992) 371–374.
[126] V.P. Antropov, M.I. Katsnelson, M. van Schilfgaarde, B.N. Harmon, Phys. Rev. Lett. 75 (1995) 729.
[127] O.N. Myrasov, V.A. Gubanov, A.I. Liechtenstein, Phys. Rev. B 45 (1992) 12330.
[128] G.M. Stocks, B. Ujfalussy, X. Wang, D.M.C. Nicholson, W.A. Shelton, Y. Wang, A. Canning, B.L. Györffy, Phil. Mag. B 78 (1998) 665.
[129] T.C. Schulthess, W.H. Butler, G.M. Stocks, S. Maat, G.J. Mankey, J. Appl. Phys. 85 (1999) 4842.
[130] G.M. Stocks, W.A. Shelton, T.C. Schulthess, B. Ujfalussy, W.H. Butler, A.J. Canning, Appl. Phys. 91 (2002) 7355.
[131] O.N. Mryasov, J. Magn. Magn. Mater. 272-276 (2004) 800.
[132] G. Brown, B. Kraczek, A. Janotti, T.C. Schulthess, G.M. Stocks, D.D. Johnson, Phys. Rev. B 68 (2003) 052405.
[133] B. Ujfalussy, L. Szunyogh, P. Bruno, P. Weinberger, Phys. Rev. Lett. 77 (1996) 1805.
[134] R. Tyer, W.M. Temmerman, Z. Szotek, G. Banach, A. Svane, L. Petit, G.A. Gehrig, Euro. Phys. Lett. 65 (2004) 519.
[135] T.C. Schulthess, W.M. Temmerman, Z. Szotek, W.H. Butler, G.M. Stocks, Nature Mater. 4 (2005) 838.
[136] A. Canning, B. Ujfalussy, T. C. Schulthess, X. –G. Zhang, W. A. Shelton, D. M. C. Nicholson, G. M. Stocks, Y. Wang, T. Dirks, IEEE Comp. Soc. Proceedings of the International Parallel Dist. Process. Symposium, 2003.
[137] B. Ujfalussy, T.C. Schulthess, G.M. Stocks, First principles calculations of the magnetic structure in FeMn/Co bilayers, in: D.P. Landau, S.P. Lewis, H. -B. Schüttler (Eds.), Computer Simulation Studies, Condensed Matter Physics, 2003 p. 43.
[138] W.E.X.-P. Wang, SIAM J. Numer. Anal. 38 (2000) 1647.
[139] C.H. Zhou, T.C. Schulthess, S. Torbrügge, D.P. Landau, Phys. Rev. Lett. 96 (2006) 120201.
[140] Q.A. Pankhurst, J. Connolly, S.K. Jones, J. Dobson, J. Phys. D.: Appl. Phys. 36 (2003) R167.
[141] M. Gonzales, K.M. Krishnan, J. Magn. Magn. Mater. 293 (2005) 265.
[142] Y. Bao, K.M. Krishnan, J. Magn. Magn. Mater. 293 (2005) 15.
[143] V.F. Puntes, Kannan M. Krishnan,, P.A. Alivisatos, Science, 291 (2001) 2115.
[144] Y. Bao, M. Beerman, K.M. Krishnan, J. Magn. Magn. Mater. 266 (2003) L245.
[145] P. Tartaj, M. del Puerto Morales, S. Veintemillas-Verdaguer, T. González-Carreño, C.J. Serna, J. Phys. D: Appl. Phys. 36 (2003) R182.

[146] M. Allen, D. Willits, J. Mosolf, M. Young, T. Douglas, Adv. Mater. 14 (21) (2002) 1562.
[147] T. Douglas, M. Young, Nature 393 (1998) 152.
[148] C. Liu, F. Yang, S.H. Chung, Q. Jin, Z. Han, A. Hoffmann, B. Kay, S.D. Bader, L. Makowski, L. Chen, J. Magn. Magn. Mater. 302 (2006) 47.
[149] A. Hoffmann, S.-H. Chung, S. D. Bader, L. Makowski, L. Chen, in: V. Labhasetwar, D. L. Leslie-Pelecky (Eds.), Biomedical Applications of Nanotechnology, Wiley, New York, in press.
[150] S.H. Chung, A. Hoffmann, S.D. Bader, L. Chen, C. Liu, B. Kay, L. Makowski, Appl. Phys. Lett. 85 (2004) 2971.
[151] D. Hautot, Q.A. Pankhurst, N. Kahn, J. Dobson, Proc. Roy. Soc. B,Bio. Lett. 270 (2003) S62.
[152] Y. Ke, Z.M. Qian, The Lancet Neurol. 2 (2003) 246.
[153] K. Honda, G. Casadesus, R.B. Petersen, G. Perry, M.A. Smith, Ann. N. Y. Acad. Sci. 1012 (2004) 179.
[154] J.F. Collingwood, A. Mikhaylova, M.R. Davidson, C. Batich, W.J. Streit, T. Eskin, J. Terry, R. Barrera, J. Dobson, J. Phys. Conf. Ser. 17 (2005) 54.
[155] A. Mikhaylova, M. Davidson, H. Toastmann, J.E.T. Channell, Y. Guyodo, C. Batich, J. Dobson, J. R. Soc. Interface 2 (2005) 33.
[156] R. von Helmot, J. Wecker, B. Hopzapfel, L. Schulz, K. Samwer, Phys. Rev. Lett. 71 (1993) 2331.
[157] S. Jin, T.H. Tiefel, M. McCormack, R.A. Fastnacht, R. Ramesh, L.H. Chen, Science 264 (1994) 413.
[158] A. Moreo, S. Yunoki, E. Dagotto, Science 283 (1999) 2034.
[159] K. Asai, O. Yokokura, N. Nishimori, H. Chou, J.M. Tranquada, G. Shirane, S. Higuchi, Y. Okajima, K. Kohn, Phys. Rev. B 50 (1994) 3025.
[160] H. Takagi, in: Proceedings of the International Conference On Materials and Mechanisms of Superconductivity, High Temperature Superconductors VI; Physica C 341-348 (2000) 3.
[161] J.B. Goodenough, J.S. Zhou, J. Chan, Phys. Rev. B 47 (1993) 5275.
[162] I. Affleck, J.B. Marston, Phys. Rev. B 37 (1988) 3774.
[163] Y. Maeno, T.M. Rice, M. Sigrist, Phys. Today 54 (1) (2001) 42.
[164] J.B. Goodenough, Magnetism and the Chemical Bond, Huntington, Krieger, 1976.
[165] R. Birgeneau, G. Shirane, in: D.M. Ginsberg (Ed.), Physical Properties of High Temperature Superconductors, World Scientific, Singapore, 1989.
[166] E. Dagotto, T. Hotta, A. Moreo, Phys. Rep. 344 (2001) 1.
[167] E. Dagotto, Science 309 (2005) 257.
[168] R.B. Griffiths, Phys. Rev. B 12 (1975) 345.
[169] H.J. Lee, K.H. Kim, M.W. Kim, T.W. Noh, B.G. Kim, T.Y. Koo, S.-W. Cheong, Y.J. Wang, X. Wei, Phys. Rev. B 65 (2002) 115118.
[170] M.B. Salamon, M. Jaime, Rev. Mod. Phys. 73 (2001) 583.
[171] N.D. Mathur, P.B. Littlewood, Solid. State Commun. 119 (2001) 271.
[172] N.A. Spaldin, M. Fiebig, Science 309 (2005) 391.
[173] J. Orenstein, A.J. Millis, Science 188 (2000) 468.
[174] V.K. Pecharsky, K.A. Gschneidner Jr., Phys. Rev. Lett. 78 (1997) 4494.
[175] O. Tegus, E. Brück, L. Zhang, Dagula, K. H. J. Buschow, F. R. de Boer, Physica B 319 (2002) 174.
[176] M. Jaime, P. Lin, M.B. Salamon, P. Dorsey, M. Rubinstein, Phys. Rev. B 60 (1999) 1028.
[177] C.H. Booth, F. Bridges, G.H. Kwei, J.M. Lawrence, A.L. Cornelius, J.J. Neumeier, Phys. Rev. B 57 (1998) 10440.
[178] C.H. Booth, F. Bridges, G.H. Kwei, J.M. Lawrence, A.L. Cornelius, J.J. Neumeier, Phys. Rev. Lett. 80 (1998) 853.
[179] M.B. Salamon, S.H. Chun, Phys. Rev. B 68 (2003) 014411.
[180] R.B. Griffiths, Phys. Rev. Lett. 23 (1969) 17.
[181] J. Burgy, M. Mayr, V. Martin-Mayor, A. Moreo, E. Dagotto, Phys. Rev. Lett. 87 (2001) 277202.
[182] A.J. Bray, Phys. Rev. Lett. 59 (1987) 586.
[183] T.D. Lee, C.N. Yang, Phys. Rev. 87 (1952) 410.
[184] P.J. Kortman, R.B. Griffiths, Phys. Rev. Lett. 27 (1971) 1439.
[185] M.B. Salamon, P. Lin, S.H. Chun, Phys. Rev. Lett. 88 (2002) 197203.
[186] J. Burgy, M. Mayr, V. Martin-Mayor, A. Moreo, E. Dagotto, Phys. Rev. Lett. 87 (2001) 277202.
[187] E. Dagotto, T. Hotta, A. Moreo, Phys. Rep. 344 (2001) 1.
[188] E. Dagotto, Nanoscale Phase Separation and Colossal Magnetoresistance, Springer, Berlin, 2002.
[189] C. Howald, P. Fournier, A. Kapitulnik, Phys. Rev. B 64 (2001) 100504.
[190] S.H. Pan, J.P. O'Neal, R.L. Badzey, C. Chamon, H. Ding, J.R. Engelbrecht, Z. Wang, H. Eisaki, S. Uchida, A.K. Gupta, K.-W. Ng, E.W. Hudson, K.M. Lang, J.C. Davis, Nature 413 (2001) 282.
[191] E.F. Kneller, R. Hawig, IEEE Trans. Magn. 27 (1991) 3588.
[192] H. Zeng, J. Li, J.P. Liu, Z.L. Wang, S. Sun, Nature 420 (2002) 395.
[193] E.E. Fullerton, J.S. Jiang, M. Grimsditch, C.H. Sowers, S.D. Bader, Phys. Rev. B 58 (1998) 12193.
[194] A. Hoffmann, S.G.E. te Velthuis, Z. Sefrioui, J. Santamaría, M.R. Fitzsimmons, S. Park, M. Varela, Phys. Rev. B 72 (2005) 140407(R).
[195] N. Mathur, P. Littlewood, Physics Today (Jan,) (2003) 26.
[196] S.J. Potashnik, K.C. Ku, S.H. Chun, J.J. Berry, N. Samarth, P. Schiffer. Appl. Phys. Lett. 79 (2001) 1495.
[197] J.F. Herbst, Rev. Mod. Phys. 63 (1991) 819.
[198] D. Haskel, J. Lang, Z. Islam, G. Srajer, J. Cross, P. Canfield, IEEE Trans. Mag. 40 (2004) 2874.
[199] D. Haskel, J.C. Lang, Z. Islam, A. Cady, G. Srajer, M. van Veenendaal, P.C. Canfield, Phys. Rev. Lett. 95 (2005) 217207.
[200] J.W. Freeland, K.E. Gray, L. Ozyuzer, P. Berghuis, E. Badica, J. Kavich, H. Zheng, J.F. Mitchell, Nature Mater. 4 (2005) 62.
[201] K. Horiba, M. Taguchi, A. Chainani, Y. Takata, E. Ikenaga, D. Miwa, Y. Nishino, K. Tamasaku, M. Awaji, A. Takeuchi, M. Yabashi, H. Namatame, M. Taniguchi, H. Kumigashira, M. Oshima, M. Lippmaa, M. Kawasaki, H. Koinuma, K. Kobayashi, T. Ishikawa, S. Shin, Phys. Rev. Lett. 93 (2004) 236401.
[202] H. Tanaka, Y. Takata, K. Horiba, M. Taguchi, A. Chainani, S. Shin, D. Miwa, K. Tamasaku, Y. Nishino, T. Ishikawa, E. Ikenaga, M. Awaji, A. Takeuchi, T. Kawai, K. Kobayashi, Phys. Rev. B 73 (2006) 094403.
[203] G.A. Smolenski, I.E. Chupis, Ferroelectromagnets. Usp. Fiz. Nauk. 137 (1982) 415;
G.A. Smolenski, I.E. Chupis, Ferroelectromagnets. Usp. Fiz. Nauk. Sov. Phys. Usp. 25 (1982) 475.
[204] H. Schmid, Ferroelectrics 162 (1994) 317.
[205] E. Ascher, H. Rieder, H. Schmid, H. Stössel, J. Appl. Phys. 37 (1966) 1404.
[206] J. Wang, J.B. Neaton, H. Zheng, V. Nagarajan, S.B. Ogale, B. Liu, D. Viehland, V. Vaithyanathan, D.G. Schlom, U.V. Waghmare, N.A. Spaldin, K.M. Rabe, M. Wuttig, R. Ramesh, Science 299 (2003) 1719.
[207] G.A. Smolenskii, V.M. Yudin, E.S. Sher, Yu.E. Stolypin, Sov. Phys. JETP 16 (1963) 622.
[208] M. Pasquale, C.P. Sasso, L.H. Lewis, L. Giudici, T. Lograsso, D. Schlagel, Phys. Rev. B 72 (2005) 094435.
[209] H. Huang, L.M. Zhou, J. Phys. D, Appl. Phys. 37 (2004) 3361.
[210] W. Prellier, M.P. Singh, P. Murugavel, J. Phys.: Condens. Mater. 17 (2005) R803.
[211] Th. Lonkai, D.G. Tomuta, U. Amann, J. Ihringer, R.W.A. Hendrikx, D.M. Többens, J.A. Mydosh, Phys. Rev. B 69 (2004) 134108.
[212] N. Hur, S. Park, P.A. Sharma, J.S. Ahn, S. Guha, S-W. Cheong,, Nature 429 (2004) 392.
[213] P.M. Platzmann, N. Tzoar, Phys. Rev. B 2 (1970) 3556.
[214] D. Gibbs, D.E. Moncton, K.L. D'Amico, J. Bohr, B.H. Grier, Phys. Rev. Lett. 55 (1985) 234.
[215] D.F. McMorrow, D. Gibbs, J. Bohr, in: K.A. Gschneidner, L. Eyring (Eds.), Handbook on the Physics and Chemistry of Rare Earths, vol. 26, Elsevier Science, Amsterdam, New York, 1999.
[216] G. Schütz, W. Wagner, W. Wilhelm, P. Kienle, R. Zeller, R. Frahm, G. Materlik, Phys. Rev. Lett. 58 (1987) 737.

[217] G. Schütz, R. Frahm, P. Mautner, R. Wienke, W. Wagner, W. Wilhelm, P. Kienle, Phys. Rev. Lett. 62 (1989) 2620.
[218] C.T. Chen, F. Sette, Y. Ma, S. Modesti, Phys. Rev. B 42 (1990) 7262.
[219] K. Namikawa, M. Ando, T. Nakajima, H. Kawata, J. Phys. Soc. Jpn. 54 (1985) 4099.
[220] D. Gibbs, D.R. Harshman, E.D. Isaacs, D.B. McWhan, D. Mills, C. Vettier, Phys. Rev. Lett. 61 (1988) 1241.
[221] J.W. Freeland, V. Chakarian, K. Bussmann, Y.U. Idzerda, H. Wende, C.-C. Kao, J. Appl. Phys. 83 (1998) 6290.
[222] C.S. Nelson, G. Srajer, J.C. Lang, C.T. Venkataraman, S.K. Sinha, H. Hashizume, N. Ishimatsu, N. Hosoito, Phys. Rev. B 60 (1999) 12234.
[223] D.R. Lee, S.K. Sinha, D. Haskel, Y. Choi, J.C. Lang, S.A. Stepanov, G. Srajer, Phys. Rev. B 68 (2003) 224409.
[224] D.R. Lee, S.K. Sinha, C.S. Nelson, J.C. Lang, C.T. Venkataraman, G. Srajer, R.M. Osgood III, Phys. Rev. B 68 (2003) 224410.
[225] J.J. Pollmann, G. Srajer, D. Haskel, J.C. Lang, J. Maser, J.S. Jiang, S.D. Bader, J. Appl. Phys. 89 (2001) 7165.
[226] J.C. Lang, J. Pollmann, D. Haskel, G. Srajer, J. Maser, J.S. Jiang, S.D. Bader, SPIE Proc 4499 (2001) 1.
[227] D. Gibbs, G. Grübel, D.R. Harshman, E.D. Isaacs, D.B. McWhan, D. Mills, C. Vettier, Phys. Rev. B 43 (1991) 5663.
[228] C.T. Chen, Y.U. Idzerda, H.-J. Lin, N.V. Smith, G. Meigs, E. Chaban, G.H. Ho, E. Pellegrin, F. Sette, Phys. Rev. Lett. 75 (1995) 152.
[229] D. Gibbs, J.P. Hill, C. Vettier, Phys. Stat. Sol. (B) 215 (1999) 667.
[230] D.B. McWhan, J. Synch. Rad 1 (1994) 83.
[231] G. van Der Laan, B.T. Thole, G.A. Sawatzky, J.B. Goedkoop, J.C. Fuggle, J.-M. Esteva, R. Karnatak, J.P. Remeika, Phys. Rev. B 34 (1986) 6529.
[232] J. Stöhr, H.A. Padmore, S. Anders, T. Stammler, M.R. Scheinfein, Surf. Rev. Lett. 5 (1998) 1297.
[233] A. Scholl, J. Stöhr, J. Lüning, J.W. Seo, J. Fompeyrine, H. Siegwart, J.-P. Locquet, F. Nolting, S. Anders, E.E. Fullerton, M.R. Scheinfein, H.A. Padmore, Science 287 (2000) 1014.
[234] J.C. Lang, D.R. Lee, D. Haskel, G. Srajer, J. Appl. Phys. 95 (2004) 6537.
[235] B.T. Thole, P. Carra, F. Sette, G. van der Laan, Phys. Rev. Lett. 68 (1992) 1943.
[236] P. Carra, B.T. Thole, M. Altarelli, X. Wang, Phys. Rev. Lett. 70 (1993) 649.
[237] S.-B. Choe, Y. Acremann, A. Scholl, A. Bauer, A. Doran, J. Stöhr, H.A. Padmore, Science 304 (2004) 420.
[238] K. Harkay, M. Borland, Y.-C. Chae, G. Decker, R. Dejus, L. Emery, W. Guo, D. Horan, K.-J. Kim, R. Kustom, D. Mills, S. Milton, A. Nassiri, G. Pile, V. Sajaev, S. Shastri, G. Waldschmidt, M. White, B. Yang, A. Zholents, Proc. 2005 Part. Accel. Conf. (2005) 668.
[239] S.-K. Kim, J.B. Kortright, Phys. Rev. Lett. 86 (2001) 1347.
[240] S.-H. Yang, B.S. Mun, N. Mannella, S.-K. Kim, J.B. Kortright, J. Underwood, F. Salmassi, E. Arenholz, A. Young, Z. Hussain, M.A. Van Hove, C.S. Fadley, J. Phys. Condens. Matter. 14 (2002) L406.
[241] C.S. Fadley, Nucl. Instrum. Methods. A 547 (2005) 24.
[242] Issue dedicated to standing wave studies of surfaces and interfaces, Synch. Rad. News 17(3) 2004.
[243] J.B. Kortright, D.D. Awschalom, J. Stöhr, S.D. Bader, Y.U. Idzerda, S.S.P. Parkin, I.K. Schuller, H.-C. Siegman, J. Magn. Magn. Mater. 207 (1999) 7.
[244] J.B. Kortright, S.-K. Kim, G.P. Denbeau, G. Zeltzer, K. Takano, E.E. Fullerton, Phys. Rev. B 64 (2001) 092401.
[245] J.B. Kortright, O. Hellwig, D.T. Margulies, E.E. Fullerton, J. Magn. Magn. Mater. 240 (2001) 325.
[246] O. Hellwig, D.T. Margulies, B. Lengsfield, E.E. Fullerton, J.B. Kortright, Appl. Phys. Lett. 80 (2002) 1234.
[247] E.E. Fullerton, O. Hellwig, Y. Ikeda, B. Lengsfield, K. Takano, J.B. Kortright, IEEE Trans. Mag. 38 (2002) 1693.
[248] A. Hoffmann, M.R. Fitzsimmons, J.A. Dura, C.F. Majkrzak, Phys. Rev. B 65 (2002) 024428.
[249] C. L'abbé, J. Meersschaut, W. Sturhan, J.S. Jiang, T.S. Toellner, E.E. Alp, S.D. Bader, Phys. Rev. Lett. 93 (2004) 037201.
[250] M.R. Fitzsimmons, S.D. Bader, J.A. Borchers, G.P. Felcher, J.K. Furdyna, A. Hoffman, J.B. Kortright, I.K. Schuller, T.C. Schulthess, S.K. Sinha, M.F. Toney, D. Weller, S. Wolf, J. Magn. Magn. Mater. 271 (2004) 103.
[251] S. Roy, M.R. Fitzsimmons, S. Park, M. Dorn, O. Petracic, I.V. Roshchin, Z.-P. Li, X. Batlle, R. Morales, A. Misra, X. Zhang, K. Chesnel, J.B. Kortright, S.K. Sinha, I.K. Schuller, Phys. Rev. Lett. 95 (2005) 047201.
[252] 〈http://www.esrf.fr/NewsAndEvents/Spotlight/spotlight1_volpe/〉.
[253] N. Mannella, A. Rosenhahn, C.H. Booth, S. Marchesini, B.S. Mun, S.H. Yang, K. Ibrahim, Y. Tomioka, C.S. Fadley, Phys. Rev. Lett. 92 (2004) 166401.
[254] C.S. Fadley, in: R.Z. Bachrach (Ed.), Synchrotron Radiation Research: Advances in Surface and Interface Science, Plenum Press, New York, 1992.
[255] B.D. Hermsmeier, J. Osterwalder, D.J. Friedman, B. Sinkovic, T. Tran, C.S. Fadley, Phys. Rev. B 42 (1990) 11895.
[256] A.P. Kaduwela, Z. Wang, S. Thevuthasan, M.A. Van Hove, C.S. Fadley, Phys. Rev. B Rapid Commun. 50 (1994) 9656.
[257] S.-H. Yang, C.S. Fadley, B.S. Mun, Synch. Rad. News 17 (2004) 24.
[258] S.B. Wilkins, P.D. Hatton, M.D. Roper, D. Prabhakaran, A.T. Boothroyd, Phys. Rev. Lett. 90 (2003) 187201.
[259] S.-H. Yang, B.S. Mun, A.W. Kay, S.K. Kim, J.B. Kortright, J.H. Underwood, Z. Hussain, C.S. Fadley, Surf. Sci. Lett. 461 (2000) L557.
[260] M. Tegze, G. Faigel, Nature 380 (1996) 49.
[261] T. Gog, P.M. Len, G. Materlik, D. Bahr, C. Sanchez-Hanke, C.S. Fadley, Phys. Rev. Lett. 76 (1996) 3132.
[262] G. Faigel, M. Tegze, Rep. Prog. Phys. 62 (1999) 355.
[263] C.S. Fadley, M.A. Van Hove, A. Kaduwela, S. Omori, L. Zhao, S. Marchesini, J. Phys.: B Condens. Matter. 13 (2001) 10517.
[264] M. Tegze, G. Faigel, S. Marchesini, M. Belakhovsky, A.I. Chumakov, Phys. Rev. Lett. 82 (1999) 4847.
[265] S. Omori, Y. Nihei, E. Rotenberg, J.D. Denlinger, S. Marchesini, S.E. Kevan, B.P. Tonner, M.A. Van Hove, C.S. Fadley, Phys. Rev. Lett. 88 (2002) 055504.
[266] Y. Takahashi, K. Hayashi, E. Matsubara, Phys. Rev. B 71 (2005) 134107.
[267] J.-M. Bussat, C.S. Fadley, Z. Hussain, A.W. Kay, G. Lebedev, B.A. Ludewigt, G. Meddeler, A. Nambu, M. Press, H. Speiler, B. Turko, M. West, G. Zizka, AIP Conf. Proc. 705 (2004) 945.
[268] A. Nambu, J.-M. Bussat, M. West, B.C. Sell, M. Watanabe, A.W. Kay, N. Mannella, B.A. Ludewigt, M. Press, B. Turko, G. Meddeler, G. Zizka, H. Speiler, H. van der Lippe, P. Denes, T. Ohta, Z. Hussain, C.S. Fadley, J. Elec. Spec. Rel. Phen. 137 (2004) 691.